ALTERNATIVE FUELS AND CHEMICALS FROM SYNTHESIS GAS

FINAL

Quarterly Status Report

For the Period 1 April - 30 June 1996 --#7

Contractor

AIR PRODUCTS AND CHEMICALS, INC.
7201 Hamilton Boulevard
Allentown, PA 18195-1501

Prepared for the United States Department of Energy
Under Contract No. FC22-95PC93052--29
Contract Period 29 December 1994 - 28 December 1997

January 1999

NOTE: THIS DOCUMENT HAS BEEN CLEARED OF PATENTABLE INFORMATION

DISCLAIMER

Alternative Fuels and Chemicals from Synthesis Gas

Quarterly Technical Progress Report

1 April - 30 June 1996

Contract Objectives

The overall objectives of this program are to investigate potential technologies for the conversion of synthesis gas to oxygenated and hydrocarbon fuels and industrial chemicals, and to demonstrate the most promising technologies at DOE's LaPorte, Texas, Slurry Phase Alternative Fuels Development Unit (AFDU). The program will involve a continuation of the work performed under the Alternative Fuels from Coal-Derived Synthesis Gas Program and will draw upon information and technologies generated in parallel current and future DOE-funded contracts.

Summary of Activity

- Work continued through the quarter on the modifications for the Fischer-Tropsch III (F-T III) run at LaPorte. Instrumentation specification began, including slurry/wax flow meters, differential pressure transmitters, and automatic shutoff valves. Operability reviews were conducted both internally and with Shell personnel. Automatic shutdown and flush scenarios were developed and engineered. A list of desired signals to be connected to Shell's high-speed data acquisition system was developed. A P&ID review meeting was held, and the updated flow sheet was approved for the run.

  The demonstration plans were presented at a review meeting with DOE on 18 April. Objectives, run plan outline, scope of modifications, maximum production rates and project schedule were discussed at the meeting.

  In May, Karen Jones of Radian completed her initial evaluation of the air emission issues for F-T III. Although there is a net decrease in emissions compared to F-T II, there are instances of individual increases in component emissions. For example, F-T III has higher hourly CO emissions from process equipment because the CO concentration is higher in the reactor effluent due to lower conversion. Also, VOCs are higher for HC loading fugitives due to the catalyst selectivity difference. Upon recommendation from Radian, an exemption application has been drafted and will be filed with the Texas Natural Resources Conservation Commission (TNRCC). Now that the AFDU is an independent facility for air emissions purposes, a significant margin has been added to each component for future flexibility. Radian does not expect any problems in having the exemption granted since we are below the exemption limitations.

  An exemption application for the air emission permit was completed in June and submitted to TNRCC. Action from TNRCC is expected within 30 to 45 days. Significant progress was made at contractual meetings between Shell, DOE and Air Products for the F-T III run. Parallel technical discussions will begin shortly to finalize the run plan.

- Another three aluminum phosphate samples, AP03, AP04, and AP05, exhibited good activity, stability, and no negative effect on the methanol catalyst in standard LPDME runs. The methanol equivalent productivity of the dual catalyst system containing AP05 was as high as 94% of the initial productivity of the dual catalyst system containing alumina.

- A LPDME life run using the new dehydration catalyst, AP05, was stopped after 934 hours on stream. Catalyst activity remained much higher than the standard system. However, the methanol catalyst showed increased deactivation in the latter part of the run (after 600 hours). Efforts are being made to understand a) if this is an experimental artifact, b) if not, what the real cause is, and c) if this deactivation pattern holds for the systems containing other AP series dehydration catalysts.

- Four more LPDME runs using three UCI bifunctional DME catalysts were conducted. The best catalyst showed a methanol equivalent productivity of 17.7 mol/kg-hr, and much better stability than the γ-alumina containing dual catalyst system. Thus, while the performance of these catalysts is improving, the performance of the best UCI catalyst is still far below that of the AP series.

- The performance of aluminum phosphate dehydration catalysts continues to show a strong dependence on the preparation parameters, including the Al/P ratio, the concentration of starting solution, final pH during precipitation, washing schemes, and the ramp rate during calcination. A systematic study of these preparation variables is underway. For example, doubling the concentration of substrate in the preparation of AP04 and AP05 lead to a catalyst with considerably reduced stability compared with the previous preparation. Successful catalyst scaleup depends upon our understanding these sensitivities.

- At Aachen, a new catalyst system, $ZrO_2/ZnO/Cu_2O/K_2O$, shows higher activity to isobutanol at low temperatures. At 400°C, this catalyst system, which has not yet been optimized, showed over twice the activity of the standard system.

- CSTR experiments at Aachen in May showed that isobutanol yield increased almost linearly with increasing residence time and catalyst loading. This information indicates that isobutanol production is not near equilibrium (in agreement with thermodynamic calculations). Aging of the Cu/Zr/Zn catalyst system which exhibited good activity at lower temperature (400°C) is under investigation. The aging pattern is currently not understood.

- The cationic complex [Rh(dppe)2]Cl, {dppe = diphenylphosphinoethane} was prepared and was found to be a good homogeneous catalyst for the carbonylation of methyl acetate to acetic anhydride. It was also found to catalyze the hydrogenation of acetic anhydride to EDDA with an activity comparable to the $RhCl_3LiI$ homogeneous system. The hydrocarbonylation of DME to EDDA with this catalyst was also successful, although with less activity than the Reillex material. It was also found that Air Products' method of preparing Rh on Reillex catalyst can give higher rhodium loadings compared to other in-situ methods reported in the literature.

- In earlier reports, Eastman indicated that in its acetic acid activation process, a small amount of a substance was generated that poisoned the subsequent desired hydrogenation of the activated acetic acid. Eastman has now found that the generation rate of this poison in the microscale lab reactors used for acetic acid activation in these experiments was nearly an order of magnitude higher than seen in the larger scale reactors. This may mean that the original concerns regarding catalyst poisoning may be more easily overcome or of less consequence than thought earlier. Reactors have been reconfigured, and tests are underway to ascertain whether the lower level of the reversible poison has significant consequences on the operation.

  During May, Eastman examined the effect of catalyst inhibitors and poisons on the conversion of activated acetic acid to acetaldehyde. The key inhibitor is reversible and the reactor can be run, albeit at lower rates in its presence, providing it is not present in overwhelming concentrations.

  During June, Eastman continued to examine the hydrogenation of activated acetic acid and the effect of poisons/inhibitors in the absence of diluent gases (nitrogen). The inhibition by the most common poison, carbon monoxide, was found to be reversible in the last two months. This inhibition could be overcome by simply raising the hydrogenation temperature to attain the same rates as in the complete absence of CO.

- The concept of adding a blend of oxygenated compounds to diesel fuel in order to enhance the cetane value and cold start properties of the fuel is being investigated. The blend of oxygenated compounds is derived from dimethyl ether chemistry, and builds on work conducted earlier in the Alternative Fuels I program, in which we examined mixed ethers as octane enhancers.

  Initial cetane number (CN) testing of a three-component composition of 1,2-dimethoxy ethane, 1,1-dimethoxy methane and methanol blended with diesel fuel showed a 40% increase in the CN of the diesel fuel when the blend was 50/50.

- Construction of the Alternative Fuels Field Test Laboratory was completed. A test run of 250 hours was successfully made, with nominal methanol yield and catalyst behavior after an initial break-in period with high carbonyls.

  Testing of the suitability of the process stream for the LPMEOH™ process began in May at Kingsport. Thus far, the gas quality presents no problems. The catalyst aging is as expected from previous laboratory experience. The Alternative Fules Field Test Laboratory was set up at the Kingsport site with no trouble.

Testing of the suitability of the process stream for the LPMEOH™ process concluded after 28 days onstream. Eastman's syngas feeds did not contain poisons in sufficient concentrations to adversely impact catalyst stability since catalyst aging was as expected from previous laboratory experience. The unit itself performed as planned. Minor problems encountered with the automatic data transfer and the control system will be corrected when the unit returns. No unexpected poisons have been seen in the feed gas at Kingsport. The state of the art GC equipment revealed the presence of 7-15 ppm COS in the Eastman feed. Higher levels were seen directly after start-up.

- Work at Bechtel during this quarter included the following:
    - ♦ *Task 1.3, Fischer-Tropsch Support* - The final version of the topical report entitled "Fischer-Tropsch Wax/Catalyst Separation Study" was issued. This report describes the catalyst separation technique study that was conducted by Bechtel.
    - ♦ *Task 4.2, Commercial Applications (Mixed Alcohol Synthesis)* - A draft topical report on the results of the study of three scenarios for the production of gasoline blendstock ethers via liquid phase mixed alcohol synthesis (LPMAS) was issued. A summary of the study entitled "Economics of MTBE Production from Synthesis Gas" was submitted to DOE as a paper to be presented at the July 1996 First Joint Power and Fuel Systems Contractors Conference.
    - ♦ *Task 4.5, Syngas Generation and Cleanup* - Information on the study to evaluate the economic incentive to develop a sulfur-tolerant methanol synthesis catalyst was provided for the first quarter 1996 report to DOE. Work on preparation of a draft report on this study, as well as the report on the identification of trace contaminants in syngas and the systems to remove them was delayed due to budget constraints and emphasis on other work.

RESULTS AND DISCUSSION

TASK 1: ENGINEERING AND MODIFICATIONS

1.1 Liquid Phase Methanol/Hydrodynamic Run - No progress to report this quarter.

1.2 Liquid Phase Fischer-Tropsch Demonstration

Work continued on the modifications for the Fischer-Tropsch (F-T) III run. Instrumentation specification began in April, including slurry/wax flow meters, differential pressure transmitters, and automatic shutoff valves. Process Engineering also started a review of existing relief devices. Operability reviews were conducted both internally and with Shell personnel. Automatic shutdown and flush scenarios were developed and engineered. A list of desired signals to be connected to Shell's high-speed data acquisition system was developed; however, the scope of this activity will be limited by costs. A Design Hazards Review was conducted on May 10. The modifications were divided into six different nodes, and a HAZOP was conducted on each node. Several issues were identified that will require follow-up. The review of existing relief devices was also completed. Due to the use of 100% hydrogen during reduction, two relief devices were found to be inadequate for this run. The reduction outlet gas will be rerouted to bypass one vessel, while the other device will be replaced. Specifications for new relief valves (PSV-236A/B and PSV-1766) and a rupture disc (PSE-1769) were issued. A P&ID review meeting was held in June, and the updated flow sheet was approved for the run.

Karen Jones of Radian completed her initial evaluation of the air emission issues for F-T III. Although there is a net decrease in emissions compared to F-T II, there are instances of individual increases in component emissions. For example, F-T III has higher hourly CO emissions from process equipment because the CO concentration is higher in the reactor effluent due to lower conversion. Also, VOCs are higher for HC loading fugitives due to the catalyst selectivity difference. Upon recommendation from Radian, an exemption application for the air emission permit was drafted. Now that the AFDU is an independent facility for air emissions purposes, a significant margin was added to each component for future flexibility. Radian does not expect any problems in having the exemption granted since we are below the exemption limitations. The exemption application was completed and submitted to TNRCC in June. Action from TNRCC is expected within 30-45 days.

The demonstration plans were presented at a review meeting with DOE on April 18. Objectives, run plan outline, scope of modifications, maximum production rates and project schedule were discussed at the meeting. Shell conducted internal reviews for the F-T III run during May. A three-way contractual meeting between Air Products, Shell, and DOE was conducted in June. Significant progress was made at this meeting. Parallel technical discussions will begin shortly to finalize the run plan.

TASK 1.3 Fischer-Tropsch Support - No progress to report this quarter.

TASK 1.4 AFDU R&D Support - No progress to report this quarter.

TASK 2: AFDU SHAKEDOWN, OPERATIONS, DEACTIVATION AND DISPOSAL

No progress to report this quarter.

TASK 3: RESEARCH AND DEVELOPMENT

3.1 New Process for DME

3.1.1 Progress in Optimizing the Performance of Aluminum Phosphate Catalysts

Four more promising aluminum phosphate dehydration catalysts, namely, AP03, AP04, AP05 and AP06 (Sample nos.1431x1-1x1, 1427x1-1x3, 1427x1-1x4, and 1429x1-1x3, respectively), have been identified. All of these samples were tested along with the BASF S3-86 methanol catalyst under the standard LPDME conditions (250°C, 750 psig, 6,000 GHSV, 80:20 methanol to dehydration catalyst ratio) using Shell gas. The criteria for a good aluminum phosphate catalyst include: 1) reasonable dehydration activity (the dehydration rate constant $k_d > 5$); 2) good stability; and 3) same deactivation rate as the methanol catalyst used in a LPMEOH™ run. As shown in Figure 3.1.1, these four samples exhibited good dehydration stability and activity, with the dehydration rate constant at about 7 after the induction period for AP03 to AP05, and about 5 for AP06. Figure 3.1.2 shows that during the entire course of the run using AP04 and for the first 700 hours of the run using AP05, the rate of methanol catalyst deactivation was within the range of methanol catalyst deactivation in LPMEOH™ lab runs. The methanol catalyst in the systems containing AP03 and AP06 experienced rapid deactivation in the first 120 hours, and then stabilized to an acceptable level. The system containing AP05, the most active of these four systems, showed a methanol equivalent activity as high as 94% of the initial activity of the standard dual catalyst system containing γ-alumina (Figure 3.1.3). The carbon-free DME selectivity of this catalyst system was 80%, as opposed to 93% in the standard dual catalyst system. It is expected that both productivity and selectivity can be improved by optimizing the ratio of the two catalysts.

Figure 3.1.2 shows that the rate of methanol catalyst deactivation for the AP05-containing system increased with time on stream, reaching an unacceptable level above 700 hours on stream. The dehydration catalyst also appeared to deactivate at the very end of the run. None of the common deactivation mechanisms explains the increase in deactivation rate with time on stream. Efforts are being made to understand a) if the deactivation is an experimental artifact, b) if not, what the real cause is, and c) if this deactivation pattern holds for the systems containing other AP series dehydration catalysts.

Figure 3.1.1 Methanol Dehydration Rate Constant as a Function of Time on Stream

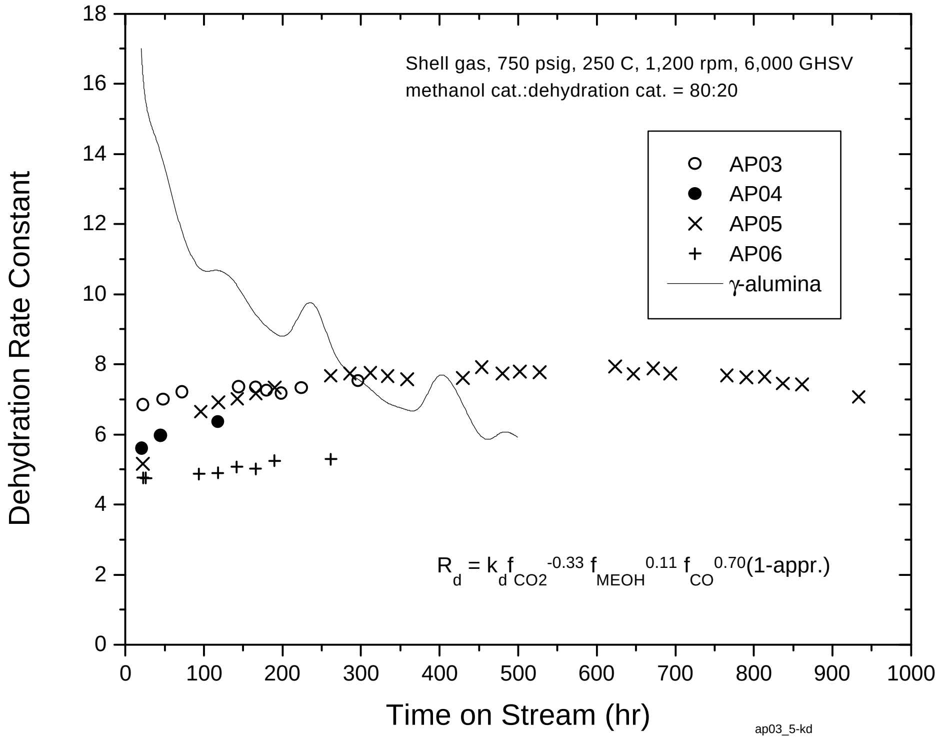

Figure 3.1.2 Normalized Methanol Rate Constant as a Function of Time on Stream

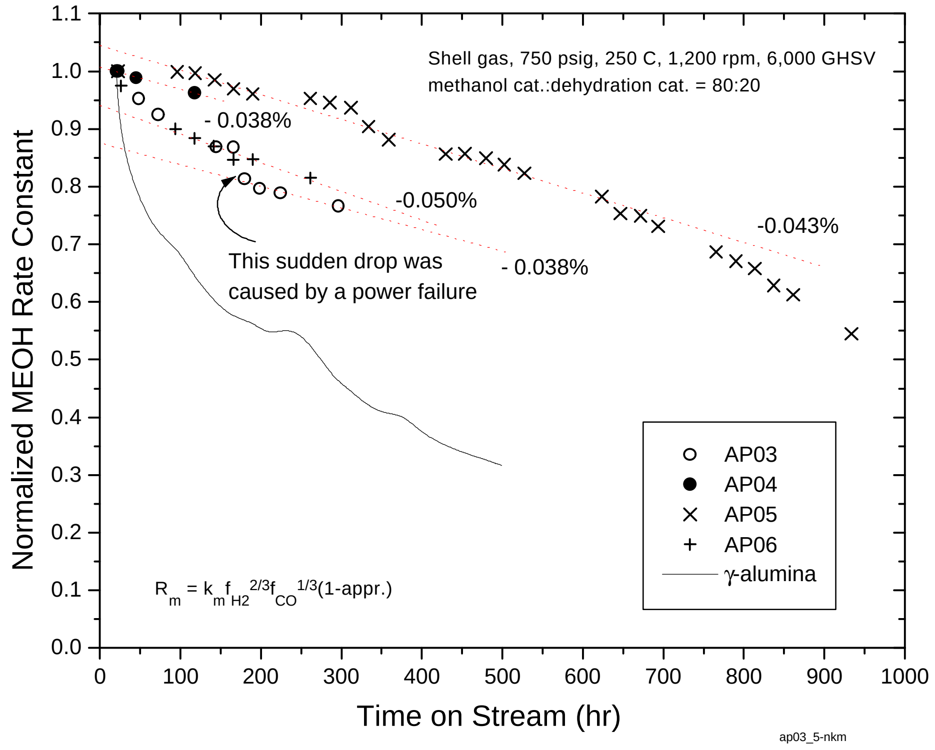

Figure 3.1.3 Methanol Equivalent Productivity as a Function of Time on Stream

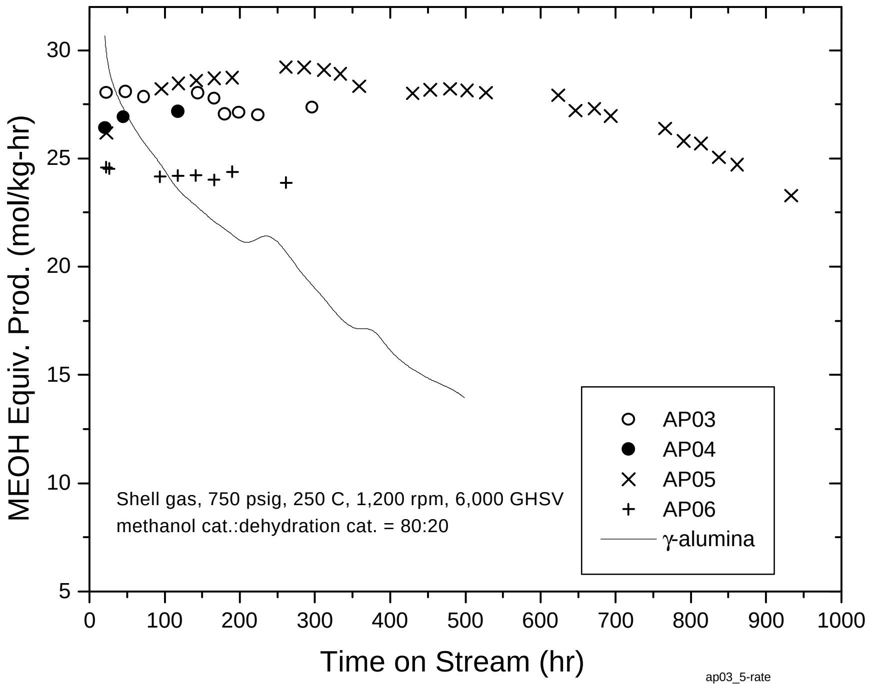

Table 3.1.1 summarizes our progress in optimizing the performance of the aluminum phosphate catalyst.

Table 3.1.1 Summary of the Performance of Dual Catalyst Systems Containing Different Aluminum Phosphate Samples

Dehydration Catalyst	**Sample No.**	**Methanol Equiv. Prod. (mol/kg-hr)**	**DME CO_2 Free Carbon Selectivity (%)**	**Stability of S3-86 (%k_m/hr)**	**Stability of Dehydration Catalyst**	**Al:P**
AP01	1407x1-1x1	24.6	69	0.032	stable	1.04
AP02	1416x1-1x1	26.2	77	0.049	stable	1.22
AP03[a]	1431x1-1x1	28.0	78	0.038	stable	3.07
AP04	1427x1-1x3	27.2	73	0.038	stable	1.66
AP05[b]	1427x1-1x4	29.1	80	0.043	stable	1.62
AP06[a]	1429x1-1x3	24.5	64	0.050	stable	2.1
γ-alumina		31[c]	93[c]	0.086[d]	rapid deact'n	--

a. Neglecting the initial rapid deactivation.
b. Based on the first 700 hours on stream.
c. Initial performance.
d. The rate of long-term deactivation.

3.1.2 Parametric Studies of Aluminum Phosphate Preparation

Efforts were continued to understand how the performance of aluminum phosphate catalysts is related to preparation parameters. The standard preparation procedure includes preparing a solution containing H_3PO_4 and $Al(NO)_3$ with the desired aluminum-to-phosphorous ratio; precipitating the solution with NH_4OH to a final pH of 9; filtrating the precipitates; washing the filter cake with water once, drying it at 110°C, and then calcining it at 650°C. Among the variables studied in the past quarter were aluminum-to-phosphorous ratio (Al/P), washing scheme, heating ramp and final temperature for calcination, and final pH during precipitation. The focus was on the effect of the aluminum phosphate catalyst on the stability of the methanol catalyst under LPDME conditions. However, no clear pattern emerged.

Al/P Ratio

Table 3.1.2 summarizes dehydration activity, methanol equivalent productivity, and methanol catalyst stability as a function of Al/P for four aluminum phosphate samples prepared by standard procedures. No trends can be observed in terms of dehydration activity and productivity as a function of the Al/P ratio. The methanol catalyst in the systems containing two samples with Al/P ratios of 2.1 and 3.0, respectively, showed two stages of deactivation: a rapid deactivation in the first 120 hours on stream and a slower long-term deactivation (compare Figure 3.1.2). The systems containing two samples with lower Al/P ratios did not show this two-stage deactivation pattern. With the initial deactivation rate for the two samples with a larger Al/P ratio, it appears that the higher Al/P ratio results in more rapid deactivation of methanol catalyst. However, with the long-term deactivation rate, the methanol catalyst is actually more stable when used with the 3.0 ratio sample than with the 2.1 ratio sample. Therefore, no simple correlation exists between the performance of the catalyst and the Al/P ratio.

Table 3.1.2 Catalyst Performance versus Al/P Ratio

Sample ID	Al/P Ratio	Dehydration Activity, k_d	MEOH Equiv. Prod. (mol/kg-hr)	Stability of MEOH Catalyst (slope)
1416x1-1x1 or AP02	1.2	6.8	26.2	-0.049%
1427x1-1x1	1.6	8.0	29.0	-0.071%
1429x1-1x1	2.1	6.3	26.0	-0.14%[a], -0.062%[b]
1431x1-1x1 or AP03	3.0	7.5	27.5	-0.19%[a], -0.038%[b]

a. Initial deactivation rate.

b. Deactivation rate after the first 120 hours on stream.

Washing Scheme

One of our hypotheses on the negative effect of aluminum phosphate catalysts on methanol catalyst stability is that the impurities in the phosphate, for example, mobile P- or Al-containing species, may contaminate the methanol catalyst under LPDME conditions. More thorough washing is an apparent answer if this indeed is the problem. We used this approach on a sample with an Al/P ratio of 1.64 (no.1427x1). The filter cake was washed with water two additional times after it had been dried at 110°C and then normally calcined at 605°C. The resulting material was AP04, which led to much better methanol catalyst stability than the sample without this extra wash (sample 1427x1-1x1 in Table 3.1.2).

However, extra washing did not result in a stable methanol catalyst in other instances. Samples 1432x1-1x4 and 1442x1-1x2 were prepared by washing the filter cake three times, instead of the single washing in the standard preparation. Sample 1442x1-1x6 featured an additional wash of a sample prepared by standard procedures, followed by calcination at 650°C. All of these samples had a negative effect on methanol catalyst stability; the deactivation rates were 0.061, 0.11, and 0.11% hr^{-1}, respectively.

Calcination Temperature

Our hypothesis regarding impurities led us to try higher calcination temperatures, reasoning that the impurities could either be removed or fixed through high-temperature calcination. Again, mixed results were observed. Calcination at 750°C of the samples with Al/P ratios of 1.6 and 2.1 produced AP05 and AP06, respectively (compare Tables 3.1.1 and 3.1.2). Calcination at 750°C of a sample with a 3.0 Al/P ratio had little effect on methanol catalyst stability compared with the one calcined at 650°C (AP03). Sample 1442x1-1x3 was prepared by final calcination at 750°C, but the methanol catalyst was not stable, having a deactivation rate of 0.082% hr^{-1} when used with this sample.

Other Parameters

Other parameters we have used include: final pH (sample 1407x4-1x1, final pH equal to 7) and ramp rate during calcination (sample 1416x1-1x4, 2°C/min. vs. normal 10°C/min.). Both samples resulted in poor methanol catalyst stability. The concentration of starting solutions was not kept consistent in the preparations discussed above. This may well be another significant parameter.

In summary, more work is needed to understand the relationship between catalyst performance and preparation. This includes more characterization of the properties of different samples. Elemental analysis has not revealed any correlations. XPS experiments show that all samples are very pure, and the surface composition is very close to the bulk one. Our current focus is characterization of the acid properties of different catalyst samples.

Other Phosphate Samples

Phosphoric Acid Doped g-Alumina

Several phosphoric acid doped Catapal B γ-alumina samples have been prepared by incipient wetness impregnation as a variation of the bulk aluminum phosphate catalyst. Two samples of different acid loadings, 3 and 25 wt%, respectively, were tested under the standard LPDME conditions using Shell gas (Runs 14665-78 and 14983-25). Both samples had been calcined at 650°C. Figure 3.1.4 shows the performance of the 3 wt% sample (#1423x1-1x1) compared to γ-alumina and AP01. The drop in the methanol equivalent productivity for the system containing 3 wt% sample is very similar to the system containing γ-alumina. The change in the methanol synthesis and dehydration rate constants also parallels that of the γ-alumina-containing dual catalyst system well (Figures 3.1.5 and 3.1.6). The 3 wt% sample essentially performed the same as the pure γ-alumina.

Figure 3.1.4 Methanol Equivalent Productivity as a Function of Time on Stream

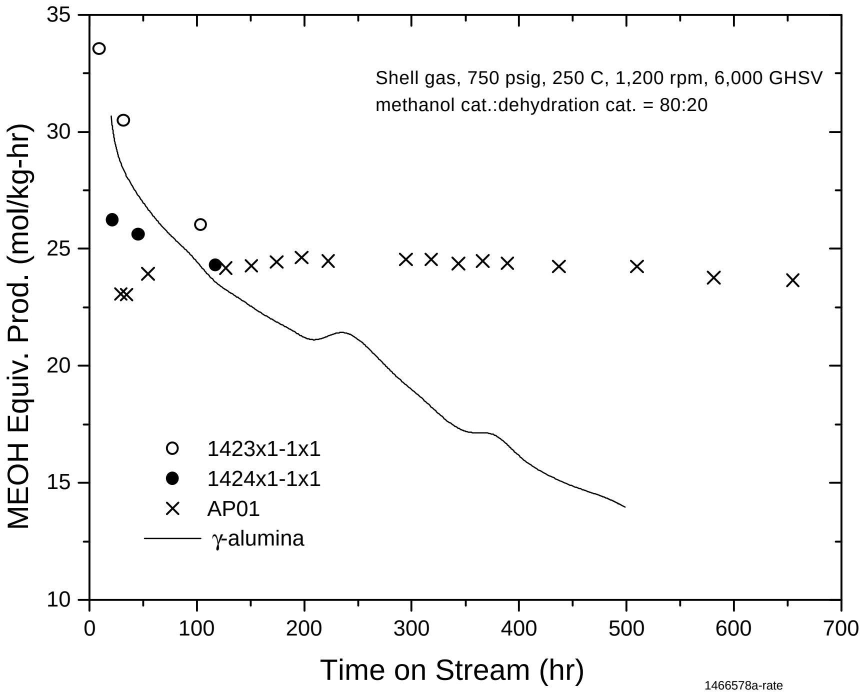

Figure 3.1.5 Methanol Synthesis Rate Constant as a Function of Time On Stream

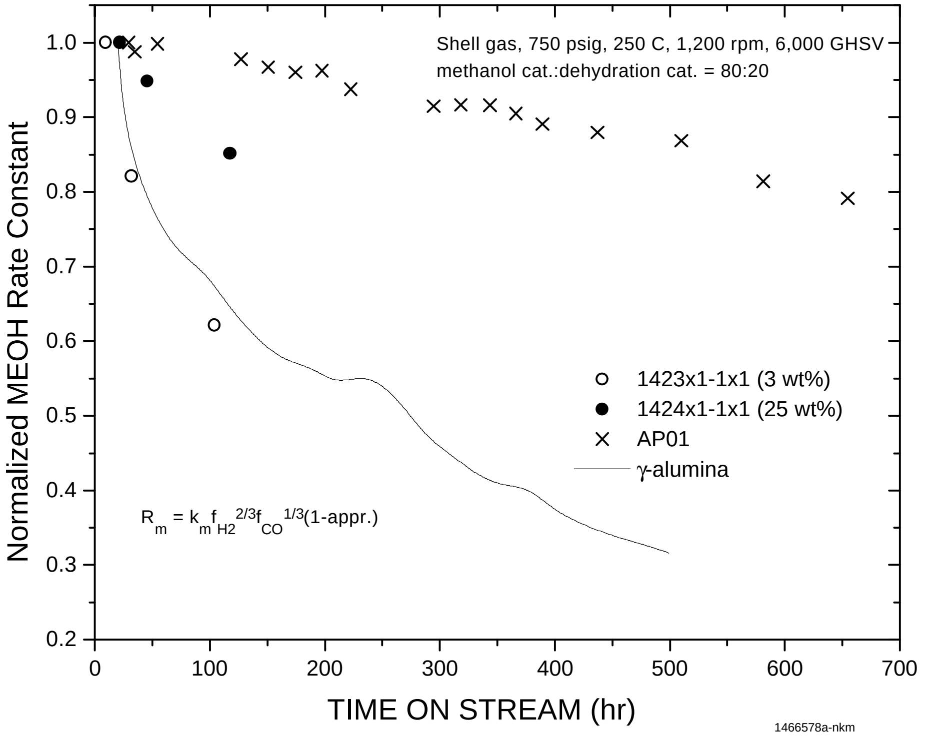

Figure 3.1.6 Methanol Dehydration Rate Constant as a Function of Time On Stream

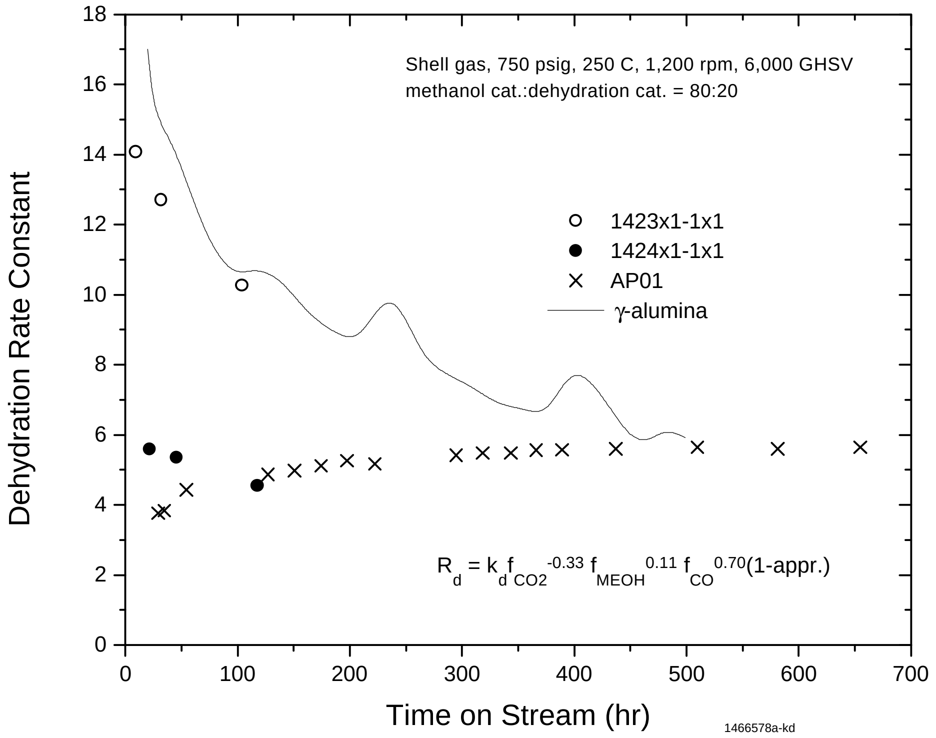

At high loading (25 wt%), the doped sample behaved more like bulk aluminum phosphate (e.g., AP01) in terms of dehydration activity and total productivity (Figures 3.1.4 and 3.1.6). However, the stability of both methanol synthesis and dehydration catalysts in this system was poor, as shown in Figures 3.1.5 and 3.1.6.

Mixed Aluminum Boron Phosphate

A mixed aluminum and boron phosphate sample (#1444x1-1x1) was prepared and tested in a LPDME run (Run 15198-01). Both methanol and dehydration catalysts showed very poor activity.

Bifunctional DME Catalysts from United Catalysts, Inc. (UCI)

The types of catalysts UCI is developing are different from dual catalyst systems we have worked with thus far. Instead of physically mixing a methanol synthesis catalyst and a dehydration catalyst in their final and active form, UCI derives the methanol synthesis and dehydration functionalities in the their catalyst from the precursor materials. That is, the catalyst is prepared by starting with the precursors of methanol synthesis and dehydration catalysts, and the resulting material is a single catalyst with both methanol synthesis and dehydration functionalities. In this way, harmony between the two types of active sites may be attained by either the formation of thermodynamically metastable materials or simply the physical fixation of submicron or nanometer domains of the two catalysts in a single micron size particle. UCI has extensive experience in methanol synthesis catalysts. Their challenge is to introduce a dehydration functionality into the methanol catalyst, yet still maintain good catalyst stability.

A number of catalyst samples were recently received from UCI. They were made using the procedures for UCI’s current methanol catalysts. However, a dehydration component or its precursor was added in the starting solution. Five of these samples were tested in a 50-cc microclave reactor under typical LPDME conditions, and the results are listed in Table 3.1.3.

Table 3.1.3 Summary of the UCI Catalyst Performance

Catalyst	Run	Methanol Equiv. Prod. (mol/kg-hr)	DME (CO_2 Free Carbon) Selectivity (%)	Stability of Methanol Functionality (-%km0/hr)	Stability of Dehydration Functionality (-%kd0/hr)
R1412-0001A	14047-75	7.1	73	0.18	0.66
R1412-000T	14047-77	15.4	53	0.36	0.89
R1412-000F	14047-79	13.9	8	0.06	0.07
R1412-000F-400 °C	14047-83*	17.7	57.3	0.09	0.06
R1412-000F-500 °C	14667-47*	17.6	53.7	0.09	0.06
R1412-0003	14667-45	16.2	30.3	0.24	0.37
R1412-0004A	14667-50	12.5	4.0	n.a.	n.a.
LPMEOH	**average**	**16**	**n.a.**	**0.14**	**n.a.**
LPDME	**average**	**32**	**91**	**0.31**	**0.25**
Target		**32**	**91**	**0.14**	**stable**

*The data of the initial sharp deactivation were excluded in the calculations.

Reaction conditions: 250°C, 750 psig, 6,000 GHSV, Shell gas, 50 cc microclave. For the LPDME runs using the dual catalyst system, the ratio of S3-86 methanol catalyst to g-alumina is 80:20.

Several criteria were used to evaluate the catalysts: methanol equivalent productivity, DME selectivity, and stability. Since a catalyst of this type contains both methanol synthesis and dehydration functionalities, which may or may not be interrelated, the stability of the catalyst was evaluated by that of each functionality. Catalyst stability of the catalyst was measured in the normal way, by the slope of the graph of the normalized rate constant plotted against time. The rate constants were calculated using the kinetic models for the dual catalyst system, as shown below:

Methanol synthesis reactions: $R_m = k_m f_{H_2}^{2/3} f_{CO}^{1/3}(1 - appr.)$ [mol/kg-cat./hr]

Methanol dehydration reaction: $R_d = k_d f_{CO_2}^{-0.33} f_{MEOH}^{0.11} f_{CO}^{0.70}(1 - appr.)$ [mol/kg-cat./hr]

where *appr.* stands for the approach to reaction equilibrium. The catalyst weight was proportioned between the methanol synthesis catalyst and the methanol dehydration catalyst based on the weight percent of the dehydration component in the starting solution. A rate constant was calculated based on the weight of the corresponding portion of the catalyst. The results from typical LPMEOH and LPDME runs (using γ-alumina) in the 50-cc microclave were included in the table for comparison. The targets for UCI catalysts were set according to the initial activity of the dual catalyst system containing γ-alumina and the stability of a methanol catalyst when used by itself.

Table 3.1.2 shows that none of these catalysts was close to the targeted performance in productivity and DME selectivity. However, catalyst R1412-000F showed some interesting behavior. This catalyst was tested in three different forms: as received and after calcination at 400 and 500°C. All three forms exhibited excellent stability in both functionalities. The rate constant data showed that the methanol synthesis activity of this catalyst was similar to that of commercial methanol catalysts (e.g., BASF S3-86). Calcination at 400 and 500°C had little effect on methanol synthesis activity, and the catalyst in its received form exhibited very low dehydration activity. Upon calcination at 400°C, dehydration activity increased drastically, with an initial k_d equal to 5, as opposed to a nominal 6 for aluminum phosphate catalysts. However, this activity dropped significantly in the first 24 hours on stream. The stabilized dehydration activity was 3 in terms of k_d. Calcination at 500°C made little difference in dehydration activity. The total activity of this catalyst is limited by its low dehydration activity. All testing results have been fed back to UCI to provide guidelines for further development.

Aluminum Sulfate Catalysts

Experimentation during the previous quarter had shown that aluminum sulfate possesses reasonable intrinsic activity for methanol dehydration, but that surface area was too small to produce adequate performance. This quarter, two new aluminum sulfate catalysts were tested. These were prepared by adding base to an aqueous solution of aluminum sulfate, precipitating $[Al(OH)x(H_2O)y(SO_4)z]^{3-x2z+}$. The intention was to incorporate sufficient coordinated sulfate into the final, calcined product that it would act like a high-surface-area $Al_2(SO_4)_3$. The two samples tested were an “alumina-like” catalyst that had been washed with water and calcined at 650°C and an “aluminum sulfate-like” catalyst that had not been washed and was calcined at 350°C. Elemental analysis indicated that the former contained 5.64 wt % sulfur, and the latter contained 11.8 wt %; however, this does not necessarily indicate that sulfate was incorporated into the structure. Neither material gave impressive activity. Using 0.6 g of the alumina-like sample with 2.4 g of S3-86 yielded a methanol equivalent productivity of 15.9 gmol/kg-hr and DME/(MeOH+DME) of only 0.088. Under the same conditions, the sulfate-like sample yielded a methanol equivalent productivity of 14.6 gmol/kg-hr and DME/(MeOH+DME) of 0.032. Although the aluminum sulfate showed some intrinsic dehydration activity, we do not intend to pursue sulfate catalysts any further because the deactivation of both the sulfate and methanol synthesis catalysts increased greatly when a larger surface area was achieved.

Lanthanum Phosphate Catalysts

Lanthanum phosphate was prepared using the same method as is currently used to prepare the aluminum phosphate materials. In this procedure, an aqueous solution of La^{3+} and PO_4^{3-} (from phosphoric acid) is treated with base to induce precipitation. However, the phosphate precipitated immediately upon addition of phosphoric acid to the aqueous solution of La^{3+}. The subsequent addition of base appeared to change the nature of the precipitate, but it is unlikely that the material that resulted is truly analogous to the aluminum phosphates. It is probably closer in structure to the simple lanthanum phosphate salt than to the mixed lanthanum-phosphorus oxide we desired. Two samples were tested: one calcined at 600°C (in air, 3 hours) and one calcined at 750°C. Neither showed appreciable DME activity, and both appeared to be losing what little dehydration activity they possessed.

Task 3.2 New Fuels from Dimethyl Ether (DME)

3.2.1 Overall 3QFY96 Objectives

The following set of objectives appeared under Task 3.2 of the previous Quarterly Technical Progress Report No. 6:

- Continue to screen immobilized catalyst candidates for hydrocarbonylation of dimethyl ether to ethylidene diacetate.

- Continue catalyst development work on the cracking of ethylidene diacetate to vinyl acetate and acetic acid.

3.2.2 Chemistry and Catalyst Development

(i) Ionic Bound Rh to Polymer Catalyst

Thus far our primary focus has been on anchoring anionic rhodium complexes on polymers and testing them for catalytic activity. This leads to the interesting question of whether cationic rhodium complexes can be anchored the same way. The cationic complex $[Rh(dppe)_2]$+ Cl^- has been supported on alumina and reported in the literature to be an efficient catalyst for the gas phase carbonylation of methyl acetate to acetic anhydride. To the best of our knowledge, there have not been any reports on the use of this complex for hydrocarbonylation reactions or for hydrogenation reactions. We decided to test this complex as a homogeneous catalyst for the various steps involved in the conversion of DME to EDA. If the complex were active, attempts would be made to support it on thermally robust supports.

Carbonylation of Methyl Acetate to Acetic Anhydride

The reaction conditions used were similar to those reported for the Eastman Chemical acetic anhydride process. Into a 300-cc autoclave were added $[Rh(dppe)_2]^+ Cl^-$ (0.46 g), MeOAc (0.695 mol), CH_3CHI (0.074 mol), and HOAc (0.29 mol). The contents were pressurized with a 95/5 CO/H_2 mix, reacted at 190°C and 750 psi for 4 hours and then analyzed by gas chromatography. The results are compared with other catalytic runs in Table 3.2.1.

Table 3.2.1 Carbonylation of Methyl Acetate to Acetic Anhydride

Catalyst	MeOAc Conv %	Ac_2O Turnover Freq (hr-1)
Reillex 2.24%Rh	45	159
$RhCl_3$	30	99
$RhCl_3$ / LiI	77	332
$[Rh(dppe)_2]^+$	40.6	127*

* Mass balance = 91%

These initial results without optimization show that $[Rh(dppe)_2]^+ Cl^-$ is a good homogeneous catalyst for the carbonylation of methyl acetate, although not as good as the $RhCl_3$/LiI system (commercial process).

Hydrogenation of Acetic Anhydride to Ethylidene Diacetate

The reaction conditions used for hydrogenation were as follows. Into a 300-cc autoclave were added $[Rh(dppe)_2]^+ Cl^-$(0.46 g), Ac_2O (0.22 mol), CH_3I (0.063 mol), and HOAc (2.4 mol). The contents were pressurized with a 50/50 CO/H_2 mix, reacted at 190°C and 1500 psi for 4 hours and then analyzed by gas chromatography. The results are compared with other catalytic runs in Table 3.2.2.

Table 3.2.2 Hydrogenation of Acetic Anhydride to Ethylidene Diacetate

Catalyst	Ac_2O Conv %	EDA Turnover Freq (hr-1)
$RhCl_3$	58.8	7
$RhCl_3$/ LiI	85	29
Reillex 2.24%Rh	60	59
$Rh[dppe]_2{}^+$	35	30*

* Mass balance = 82%

The results show that the cationic rhodium complex is also a good hydrogenation catalyst for acetic anhydride--as good as the $RhCl_3$/ LiI system. This must mean that the coordinated phosphine ligands act as promoters.

Conversion of DME to Ethylidene Diacetate

Having demonstrated that the cationic complex $[Rh(dppe)_2]^+ Cl^-$ is an efficient carbonylation and hydrogenation catalyst, we attempted the hydrocarbonylation of DME to EDA using the following conditions: catalyst (0.5 g), HOAc (1.2 mol), DME (0.12 mol), CH_3I (0.03 mol), CO/H_2 (1:1), 1500 psi, 190°C, and 2 hours reaction time. The results showed that EDA was formed with a turnover frequency of 15 hr-1, which is lower than that of the Reillex catalyst (75 hr-1). It was also found that the complex was extremely sensitive to the head space composition above the liquid. For example, using twice the DME gave only the carbonylation product (acetic anhydride). Nevertheless, the results are encouraging enough that a heterogeneous analog of this catalyst will be prepared.

Preparation of the Anionic Reillex Catalyst in the Reactor

Until now, Reillex catalyst has been synthesized stepwise in the laboratory. First the polymer is reacted with methyl iodide to quaternize the pyridine sites. Then this solid is reacted with the dimer $Rh_2(CO)_4Cl_2$ in toluene. The iodide ion on the polymer reacts with the dimer to give $[Rh(CO)_2ICl]^-$, which is now anionically bound. Using this method, we have synthesized polymers with various loadings of rhodium. A more convenient method, that of Marston et al. of Reilly Industries, was attempted. To a 300-cc reactor were added $RhCl_3$. $3H_2O$ (0.57 g), CH_3OH (50 g), CH_3COOH (100 g), CH_3I (14.5 g), and Reillex 425 (10 g). The reactor was pressurized with CO (750 psi) at 190°C for 3 hours. In this method the $Rh(CO)_2I_3^-$ is formed in the reactor and is chemically attached to the Reillex 425. The Reillex was recovered and analyzed for rhodium, which was found to be ~0.7 wt %. If all the rhodium had incorporated, the calculated value would have been 1.2 wt %. We therefore concluded that this method is not efficient for preparing Reillex materials with a high loading of rhodium (5% and above), which our method allows.

Examples for Patent Applications

Additional experimental data were collected for a group of three patent applications. One involves the production of acetic anhydride from methyl acetate using a heterogeneous catalyst. Earlier reports described the preparation of a new catalyst consisting of a polymer containing quaternized phosphine groups anionically attached to a rhodium complex. This catalyst contained 5.4 wt % rhodium and was used for the conversion of methyl acetate to acetic anhydride. Upon the first recycle of the catalyst, no loss in activity was found. The most relevant prior art is a patent from BP (US 5360929), which uses the Reillex polymer containing quaternized pyridine groups anionically attached to a rhodium complex. To determine if there was any difference between the two catalysts, recycle experiments were performed with the Reillex materials in the methyl acetate to acetic anhydride conversion.

An autoclave was charged with methyl acetate (0.695 mol), methyl iodide (0.074 mol), acetic acid (0.29 mol), and 0.8 g of heterogeneous catalyst. The autoclave was pressured with a 95/5 mix of CO/H_2, and the reaction was run at 190°C and 750 psi for 4 hours, after which the products were analyzed by gas chromatography. The reaction was repeated with a fresh charge of reactants, and the results are shown in Table 3.2.3.

Table 3.2.3 Carbonylation of Methyl Acetate to Acetic Anhydride

Catalyst	MeOAc Conv %	Ac_2O Turnover Freq (hr^{-1})
Phosphine 5.4% Rh	34	122
Recycle	37	141
Reillex 5.1% Rh	35.8	137
Recycle	33.6	120
Reillex 2.24% Rh	51	153
Recycle	46.5	117

The results show that the phosphinated catalyst is slightly better than the Reillex material at comparable rhodium loading, and can be recycled once without loss in activity. In contrast, both the Reillex samples lost some activity when recycled. This result is quite different from that obtained for the DME to EDA conversion. That conversion employed a 50/50 CO/H_2 mix in which the Reillex polymer could be recycled three times without any apparent loss in activity, whereas the phosphinated polymer dramatically lost activity.

Safety

A safety team inspected the batch reactor and process flow system used for the DME to EDA conversion. They recommended that the relief valves be changed from 4800 to 2500 psi to be closer to the operating pressure of 1500 psi. These changes were made, and a process hazards review(PHR) was conducted. Based on the review committee recommendations, the following additional changes were incorporated:

1) The new PHR now allows increasing the DME in the reactor from 0.5 to 0.8 mol and also reducing the amount of acetic acid used. This will enable us to boost EDA productivity.
2) The maximum operating temperature has been changed from 195 to 225°C.
3) The operating procedure was rewritten, both for liquid and gas sampling.
4) The process flow diagrams were modified to be user friendly.

Synthesis of Cationic Heterogeneous Catalyst

Previously the emphasis was on using a rhodium complex $[Rh(CO)_2I_2]^-$ anionically bound to a Reillex polymer as a heterogeneous catalyst. However, no attempts were made to chemically attach a cationic rhodium complex to a polymer. The complex $[Rh(dppe)_2]^+ Cl^-$ was shown to be a good hydrocarbonylation catalyst in a homogeneous system. In order to incorporate such a complex on a polymer, a cation exchanger such as Amberlyst 15 was used. This polymer has attached sulfonic acid groups and has 4.7 mmol of exchangeable H+ per gram of polymer. To improve its poor temperature stability, we replaced the H+ with Li+. A sample of the resin was treated with LiOMe in methanol for 12 hours and filtered. The Li exchanged material was then treated with aqueous rhodium nitrate to replace some of the lithium ions with rhodium. The results of the analysis are shown in Table 3.2.4.

Table 3.2.4 Heterogeneous Cationic Hydrocarbonylation Catalyst

Sample	Rh%	Li%	Calculated Moles of H+ per 100 Grams of Polymer	Theoretical Moles of H+ per 100 Grams of Polymer
A- Li	----	2.9	41.7	47
B- Rh Li	2.53	2.46	42.8	47

Sample A-Li is the resin after the Li exchange, and gave an analysis of 2.9% Li, accounting for ~89% of the literature value of exchangeable protons. After treatment of this sample with rhodium nitrate (B-Rh Li), the lithium analysis fell from 2.9 to 2.46%, and the rhodium and Li together accounted for 91% of the exchangeable protons.

Our plan is to treat this new material with phosphine and test it as a heterogeneous catalyst. We are also considering entrapping rhodium complexes in ceramic matrices via sol gel synthesis. Work will be continued to optimize the Reillex catalytic runs and to design a lifetime test unit.

(ii) Ethylidene Diacetate to Vinyl Acetate

Background for EDA Cracking

Ethylidene diacetate (EDA) {$CH_3CH(O_2CCH_3)_2$} can be cracked to vinyl acetate (VAM) {$CH_2{=}CHO_2CCH_3$} and acetic acid (AcOH) {CH_3CO_2H}. Ethylidene diacetate (EDA) can also react to yield acetic anhydride (Ac_2O) {$(CH_3CO)_2O$} and acetaldehyde (AcH) {$CH_3C(O)H$}. Reaction 1 depicts this series.

$$Ac_2O + AcH \text{ <-------> } EDA \text{ <------> } VAM + AcOH \qquad \text{Rxn. 1}$$

Scandium Triflate

A 1-g sample of scandium triflate was loaded with a 10:1 mole ratio of Ac_2O/EDA (17.5 g Ac_2O; 2.5 g EDA) and distilled as described previously. Table 3.2.5 lists the results for this catalyst. Conversion on EDA was observed to be 89%, with a 27% selectivity to VAM. The catalyst showed 44 turnovers. A small amount of acetone was observed in the GC trace.

This experiment was repeated and examined for recycle ability. The only difference was that when 85+% of the first charge had distilled, the distillate was removed and a fresh charge of reactants added. Table 3.2.5 lists the results of the first distillate from the second experiment.

Conversion on EDA was observed to be 89% with a 29% selectivity to VAM. The catalyst showed 47 turnovers. These results were almost identical to the first experiment. The second distillate was also analyzed. Conversion on EDA was 83% with a selectivity to VAM of 56%.

Magnesium Triflate

A 1-g sample of magnesium triflate was loaded with 20 g of 10:1 mole ratio Ac_2O/EDA and distilled as described in previous quarterlies. No cracking was observed.

Lithium Triflate

A 1-g sample of lithium triflate was loaded with 20 g of 10:1 mole ratio Ac_2O/EDA and distilled as described in previous quarterlies. No cracking was observed.

Lithium Trifluoroacetate

A 1-g sample of lithium trifluoroacetate was loaded with 20 g of 10:1 mole ratio Ac_2O/EDA and distilled as described in previous quarterlies. No cracking was observed.

The number of triflates showing catalytic activity have been extended. In addition to scandium triflate, triflates of lanthanum, lutetium, and ytterbium exhibit similar activity. Results are summarized in Table 3.2.5, and a discussion of these materials follows.

Scandium Triflate

EDA Only

A 1-g sample of scandium triflate was loaded with 20 g of EDA and distilled as reported previously. The pot was allowed to distill to dryness, and the distillate was analyzed. The conversion of EDA and selectivity to VAM were calculated to be 98 and 16%, respectively. This suggests that retro-reaction to acetic anhydride and acetaldehyde is the preferred path.

5:1 Ac_2O/EDA

A 1-g sample of scandium triflate was loaded with a 5:1 mole ratio of Ac_2O/EDA (17.5 g Ac_2O; 5 g EDA) and distilled as described previously. Conversion on EDA was observed to be 89%, with a 40% selectivity to VAM. When approximately 85% of the material had been distilled, a fresh batch of feed was added. The cracking results are very similar to those observed for the initial feed. This shows the catalyst to be stable to recycle. This same catalyst charge was recycled two additional times with no apparent loss of activity.

10:1 Ac_2O/EDA

A 1=g sample of scandium triflate was loaded with a 10:1 mole ratio of Ac_20/EDA and distilled in the same manner as the previous entry. Results were similar to those observed earlier and were therefore not entered into Table 3.2.5. The selectivity for VAM was observed to be lower in the presence of higher Ac_2O concentrations. This sample had a conversion on EDA of 86% with a selectivity to VAM of 23%.

Other Triflates

Three additional triflate salts were examined. Samples of lanthanum, lutetium, and ytterbium triflate were evaluated in much the same manner as described above. All samples were evaluated with a 10:1 mole ratio of Ac_2O/EDA, and all were examined through an initial charge and three recycles.

Table 3.2.5 Cracking of Ethylidene Diacetate

Catalyst	Ac_2O/EDA Ratio	EDA Conversion (%)	VAM Selectivity (%)	Turnover #
Sc Triflate	10:1	89	27	44
Sc Triflate	10:1	89	29	47
Sc Triflate recycle	10:1	83	56	86
Sc Triflate	EDA Only	98	16	210
Sc Triflate	5:1	89	40	115
Sc Triflate recycle	5:1	85	54	150
Sc Triflate recycle	5:1	84	61	166
Sc Triflate recycle	5:1	85	57	157
La Triflate	10:1	92	29	58
La Triflate recycle	10:1	88	28	52
La Triflate recycle	10:1	83	23	41
La Triflate recycle	10:1	79	21	36
Lu Triflate	10:1	91	30	64
Lu Triflate recycle	10:1	83	27	52
Lu Triflate recycle	10:1	74	25	42
Lu Triflate recycle	10:1	75	10	17
Yb Triflate	10:1	89	22	41
Yb Triflate recycle	10:1	85	34	59
Yb Triflate recycle	10:1	85	29	50
Yb Triflate recycle	10:1	88	47	85
Sc Nafion	10:1	76	1	?

(iii) Cetane Blending Components

The addition of ethers derived from dimethyl ether to diesel fuel offers an opportunity to increase the cetane value and cold start properties of diesel fuel. Single ethers such as 1,1-dimethoxy methane or 1,2-dimethoxy ethane have cetane numbers of 55 and 101, respectively. However, blends of these components with methanol added to diesel fuel offer a potential low cost cetane enhancer composition. Such compositions are derived from the liquid product stream of a dimethyl ether oxidative coupling reactor.

In order to test this concept, the solubility of these oxygenated compounds in diesel fuel was determined experimentally. Tables 3.2.6-3.2.9 summarize observed solubility trends when the above-mentioned oxygenates were added to cyclohexane (model for diesel fuel). Table 3.2.6 shows that methanol and cyclohexane are not miscible until above 60+ vol % methanol, which is consistent with M85. When the cyclohexane is held at 70 vol %, methanol and 1,2-dimethoxy ethane can be varied over a range of compositions, and only one phase is observed (see Table 3.2.7). Also, when cyclohexane is held at 70 vol %, methanol, 1,2-dimethoxy ethane, and 1,1-dimethoxy methane can be varied over a range of compositions and remain at one phase (see Table 3.2.8). Table 3.2.9 shows that cyclohexane and 1,2-dimethoxy ethane are miscible over a wide range of compositions.

Table 3.2.6 Addition of Methanol to Cyclohexane

Components	------------------------------ Volume in ml --------------------------------							
Cyclohexane	90	80	70	60	50	40	30	20
Methanol	10	20	30	40	50	60	70	80
Phases	2	2	2	2	2	2	1	1
Top Phase	93	77	60	40	28	5		
Bottom Phase	7	23	40	60	72	95		

Table 3.2.7 Addition of 1,2-Dimethoxy Ethane and Methanol to Cyclohexane

Components	------------------------------ Volume in ml ------------------------------				
Cyclohexane	70	70	70	70	70
Methanol	20	15	10	5	0
1,2-Dimethoxy-ethane	10	15	20	25	30
Phases	1	1	1	1	1

Table 3.2.8 Addition of 1,2-Dimethoxy ethane, Methanol, and 1,1-Dimethoxy Methane to Cyclohexane

Components	------	------	Volume in ml	------	------
Cyclohexane	70	70	70	70	70
Methanol	20	15	10	5	0
1,1-Dimethoxy-methane	2	2	2	2	2
1,2-Dimethoxy-ethane	8	13	18	23	28
Phases	1	1	1	1	1

Table 3.2.9 Addition of 1,2-Dimethoxy ethane to Cyclohexane

Components	------	------	------	------	Volume in ml	------	------	------	------
Cyclohexane	9	8	7	6	5	4	3	2	1
1,2-Dimethoxy-ethane	1	2	3	4	5	6	7	8	9
Phases	1	1	1	1	1	1	1	1	1

Initially, a fuel blend of 50-75 vol % oxygenated compounds and 50-25 vol % diesel fuel is being tested at Southwest Research Institute (SwRI) for cetane and cold start properties. Two blends of oxygenated compounds were synthetically prepared at SwRI. These are:

Compound	**Mol %**	**Vol %**	**Designation**
1,2-Dimethoxy ethane	67	72.9	Product #1
methanol	7	2.9	
1,1-Dimethoxy methane	26	24.2	
1,2-Dimethoxy ethane	63.5	80.1	Product #2
methanol	33.3	16.4	
1,1-Dimethoxy methane	3.3	3.5	

Initial results regarding cetane value are reported below:

Designation	**Cetane Number (CN)**
Product #1	68.4
Product #2	27.9
Diesel Fuel	37.2
50 vol% Product #1 and 50 vol% Diesel Fuel	52.1
75 vol% Product #1 and 25 vol% Diesel Fuel	57.1

These results suggest that in the blend of 1,2-dimethoxy ethane, methanol and 1,1-dimethoxy methane, the methanol concentration should be kept low. Also, when the Product #1 composition is blended with diesel fuel at a mix of 50:50, the CN of the fuel is increased by 40%. If this correlation can be extrapolated to a Product #1 composition blended with diesel at a 25:75 mix, then the CN should be in the mid 40s. This extrapolation will be tested at SwRI.

4QFY96 Objectives
Future plans to Task 3.2 will focus on the following areas:

- Continue to screen immobilized catalyst candidates for hydrocarbonylation of dimethyl ether to ethylidene diacetate
- Continue catalyst development work on the cracking of ethylidene diacetate to vinyl acetate and acetic acid.
- Complete cetane testing at Southwest Research Institute on linear and branched dimethoxy derivatives.

Value Added Acetyls From Syngas (Eastman Chemical Company)

A. Introduction

The overall objective of this project is to produce a commercially viable process for the generation of vinyl acetate monomer (VAM) based entirely upon coal generated syngas. Previous attempts at this objective have generally involved the combination of acetic anhydride (generated by carbonylation of either dimethyl ether or methyl acetate) with acetaldehyde (generated by either hydrogenation of acetic anhydride (Ac_2O) or hydrocarbonylation of either methanol (MeOH) or a methyl ester) to generate ethylidene diacetate (EDA). The EDA is subsequently cracked to form VAM in a separate step. An exemplary process is shown below:

$$
\begin{aligned}
2\ \mathrm{CO} + 4\ \mathrm{H_2} &\longrightarrow 2\ \mathrm{MeOH} \\
2\ \mathrm{MeOH} + 2\ \mathrm{AcOH} &\longrightarrow 2\ \mathrm{AcOMe} + 2\ \mathrm{H_2O} \\
\mathrm{AcOMe} + \mathrm{CO} + \mathrm{H_2} &\longrightarrow \mathrm{AcH} + \mathrm{AcOH} \\
\mathrm{AcOMe} + \mathrm{CO} &\longrightarrow \mathrm{Ac_2O} \\
\mathrm{Ac_2O} + \mathrm{AcH} &\longrightarrow \mathrm{EDA} \\
\mathrm{EDA} &\longrightarrow \mathrm{VAM} + \mathrm{AcOH}
\end{aligned}
$$

AcH = acetaldehyde
AcOMe = methyl acetate

These efforts have failed to generate a commercially viable process to date. One of the key reasons for this failure was the very large quantities of recycled acetic acid (and consequently large commercial facilities) inherent in the earlier proposed processes.

Eastman’s proposal was to circumvent the recycle problem by generating AcH via hydrogenation of acetic acid (AcOH) instead of by reductive carbonylation. Unfortunately, this process is thermodynamically disfavored and, even if acetic acid is hydrogenated, the conditions required generally favor further hydrogenation to form ethanol and ethyl acetate, which are the thermodynamically favored products. Currently, any processes that have successfully hydrogenated a carboxylic acid circumvent this problem by operating at unacceptably high pressures and temperatures to overcome the thermodynamic constrictions and by operating at low conversion to minimize over-hydrogenation to the alcohol.

Eastman’s proposed solution to this dilemma was to convert the acetic acid to ketene (a very well known process) and utilize the high energy content of the unstable ketene intermediate to overcome the thermodynamic constrictions to hydrogenation. The key task would be to identify catalysts that hydrogenated the ketene intermediate selectively to acetaldehyde (particularly did not generate ethanol or ethyl acetate) and would do so at commercially desirable temperatures and pressures.

Several restrictions are inherent in the contemplated conversion. Due to the unstable nature of ketene, the vapor pressure of ketene in the process should be less than atmospheric and its conversion should be reasonably high. Further, recovery of acetaldehyde will require that there not be excessive amounts of additional hydrogen present. Prior to this study, no catalyst was known for accomplishing this task.

Whereas the hydrogenation of acetic acid represents the linchpin technology in the proposal, also included were some proposed advances in the subsequent conversion of acetaldehyde to VAM. Obviously, the acetaldehyde thus formed could be converted to EDA and subsequently to VAM by known methods; Eastman proposed several improvements upon this known process. However, Eastman also proposed a very speculative application of ketene for the direct esterification of acetaldehyde to yield VAM without the intermediate generation of significant amounts of EDA. If this overall speculative conversion came to fruition, the overall process would be represented by the following relatively simple scheme:

Scheme 1. Conversion of Syngas to VAM from Acetic Acid via Ketene

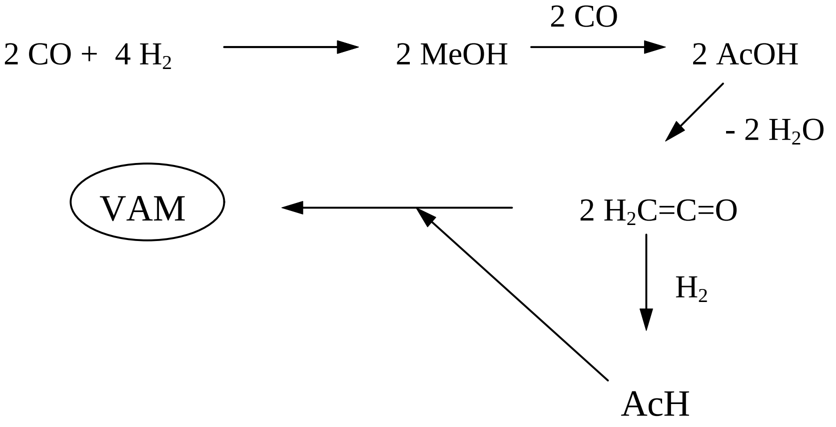

It is particularly important to point out that this scheme does not have any significant recycle loops. Further, due to the nature of the process, there are numerous opportunities to reduce capital costs through proper integration, and there is a notable economy of scale associated with the size of the intermediate steps.

Consistent with these goals, Eastman pursued the following tasks in the 2nd quarter of 1996:

Task 1.1. Examine hydrogenation of AcOH to acetaldehyde via ketene.
Task 2.1. Examine the direct conversion of AcH and ketene to VAM.
Task 3.1.a. Assess preliminary economics for a process based on ketene hydrogenation.

In addition, Eastman has been reconsidering the role reductive carbonylation of methanol (or its derivatives) might play in this process as a means of generating acetaldehyde for the process, given the success of Task 2.1.

B. Results and Discussion

General. Eastman is now operating three reactors to study ketene-based chemistry and a fourth reactor to study reductive carbonylations on a small scale. At present, two smaller scale ketene reactors are set up to separately investigate hydrogenation of ketene to acetaldehyde. (One is being used to study heterogeneous catalysts, and the other has been dedicated to surveying homogeneous catalysts.) The larger scale ketene reactor (nominally 0.6-0.8 moles/hr) is currently being used to scale up the direct conversion of acetaldehyde and ketene to VAM.

The fourth reactor, a small laboratory scale carbonylation/hydrocarbonylation unit intended to study reductive carbonylation, was set up at Eastman during this quarter. Activities such as pressure testing were completed in June, and runs are expected to commence this quarter.

Task 1.1. Hydrogenation of AcOH via Ketene Intermediates

a. Heterogeneous Catalyst Optimization Studies. In their earlier reports, Eastman described a series of Pd-based heterogeneous catalysts for the hydrogenation of ketene to acetaldehyde. As recorded in the earlier reports, these catalysts were quite effective using purified ketene and gaseous diluents, but when unpurified and undiluted ketene feeds were introduced, the hydrogenation was reversibly inhibited, likely due to carbon monoxide poisoning. Eastman has learned more about the level of carbon monoxide that caused the inhibition of the ketene hydrogenation reaction described in the January-March 1996 quarterly report.

A more accurate gas analysis technique has been developed, and Eastman has learned that the raw ketene gas generated by acetone pyrolysis contains very high levels of carbon monoxide. After the gas was scrubbed with methanol to remove the ketene, it contained 17.4% carbon monoxide. This scrubbed gas stream also contained methane (60.1%) as expected, along with small amounts of hydrogen (0.7%), carbon dioxide (0.9%) and ethane (1.7%). Thus the level of CO in the gas prepared from acetone was considerably higher than that found in a ketene stream generated by the acetic acid pyrolysis technique used industrially (about 1-3%). Eastman has learned about the performance of the ketene hydrogenation catalyst at CO levels that would typically be present in a commercial stream.

Since the amount of carbon monoxide in the raw ketene generated from acetone is so high, Eastman used the cryogenic separator to separate the bulk of the CO and other gases from the ketene and then adjusted the level of CO by blending a pure hydrogen feed with a separate fixed hydrogen-CO gas from a custom gas cylinder (containing 5% CO in hydrogen). The 5% Pd/C catalyst was used for this series of experiments since it was with this catalyst that the effect of excess CO was discovered. The following results are in chronological order, and the effect of natural catalyst deactivation must be considered along with the effect of CO.

Expt #	**% CO in H_2**	**% ketene conv.**	**HAc STY, g/(l-hr)**
1	0	93	448
2	5	58	207
3	0	76	360
4	5	20	123
5	5	28	89
6	0	48	217
7	0	47	304
8	2.5	32	149
9	2.5	29	123
10	0	50	198

The catalyst was subjected to its normal overnight hydrogenation treatment after expt. nos. 3 and 6. Even when natural deactivation is considered, the detrimental effect of CO is apparent from the above data. Actually it is somewhat surprising that the reaction proceeds at all with these high levels of CO. A vent gas analysis of the gas exiting the analytical scrubber in expt. 2 revealed that it contained 0.791% methane and 5.886% CO. It should be kept in mind that the conditions of the experiments using feed containing 5% CO in hydrogen (about 2/1 H_2/ketene ratio) are roughly equivalent to mixing a ketene stream containing about 10% CO with pure hydrogen. These data provide a rough idea of how much recycle could be tolerated in a process in which the ketene feed contained 1-3% CO.

A study was performed to determine the effect of temperature on the ability of CO to inhibit the ketene hydrogenation reaction over 5% Pd/C. The furnace used in these experiments did not allow for the control that normally exists with the steam-heated reactor (98°C). An inhibitory effect due to the presence of 5% CO was observed at 130-140°C, with the rate falling about 25%. Unfortunately the acetaldehyde selectivity dropped from 90 to 59% when the feed change was made. Neither the rate nor the selectivity returned when the CO-free feed was resumed for the next sample. No inhibitory effect was observed when the 5% CO feed was used at 158-160°C, but the acetaldehyde selectivity remained at only about 50%. At 183°C, a slight increase in the rate (but within the error normally observed) was observed when the CO-containing feed was used, but the acetaldehyde selectivity remained at about 54%. The lack of CO inhibition at higher temperatures coupled with the lowered selectivity are consistent with a large amount of the ketene decomposing to CO and methane at the higher temperatures, to the extent that the effect of the 5% CO is masked. When runs are next made at elevated temperature, vent gas samples will be taken to test this notion.

Most of Eastman's efforts have been devoted to improving material balance data for a catalyst believed to be similar to one used commercially: 3% Pd/SiO_2. This catalyst was chosen based on earlier data taken when nitrogen was present as a diluent. Under these conditions, there appeared to be an ideal combination of lifetime, rate and selectivity, and this type of catalyst should have reasonable cost and be able to survive regeneration. The plan was to perform a long-term run while taking occasional gas samples and trapping the product at -78°C to determine the amount of ethyl acetate being produced. Especially important were data obtained after the catalyst activity moderated and leveled out (hopefully at about 65-75 % conversion with a ketene/hydrogen ratio of 1/2). Some of these plans were successful, and some were not.

Ketene accountability throughout the long run with 3 % Pd/SiO_2 remained fairly close to 100%. Unfortunately, the catalyst deactivated much more rapidly when diluents were absent (ketene/hydrogen = 1/2) compared to when the diluents were present (ketene/hydrogen/nitrogen = 1/2/4). The accelerated deactivation is illustrated by Figures 3.2.1 and 3.2.2, showing rate (HAc STY) as a function of time for the same catalyst with and without diluents present. Note that the initial rates were the same. Coking may occur faster when no diluent is present. In any event, Eastman has removed the spent catalyst and is studying regeneration by calcination. Until now the catalyst has only been hydrogenated between runs to effect a partial regeneration.

The vent gas samples from the long run with 3% Pd/SiO_2 typically contained about 0.6% CO. All of the samples also contained methane (0.5-1%), and about 0.2-0.5% each of carbon dioxide, ethylene and ethane. A blank taken of the house hydrogen confirmed the absence of all of these other gases in the feed. When the ketene stream bypassed the reactor and then mixed with hydrogen, the scrubbed vent gas contained about 0.3% CO and 1% methane. These values were sufficiently close to those seen when ketene is hydrogenated that it was not possible to determine if any CO was being produced during the hydrogenation. Low levels of ethyl acetate were present in all trap samples examined, even those taken after the catalyst had lost most of its activity. Mole ratios of acetaldehyde to ethyl acetate ranged from about 120 to 240 (these numbers could be off by about 20% because the acetaldehyde levels were much higher than the gas chromatograph was calibrated for, although the ethyl acetate was in calibration range). As shown in the graph, the activity of this catalyst never leveled out in the manner anticipated. After a short period of fairly constant initial activity, the decline in activity was steady and fairly linear with time on stream until the catalyst was essentially inactive. Eastman was unable to quantify the effect of 5% CO on the performance of this catalyst because, by the time the experiment was conducted, the catalyst was almost totally inactive under any conditions. This run will be repeated with the regenerated catalyst.

b. CO Tolerant Catalysts. The advent of a CO-tolerant catalyst would simplify the process, but would also cut costs by allowing the use of less pure hydrogen (i.e., allow some carbon monoxide content). Eastman will be devoting significant efforts to identifying a CO-tolerant catalyst in the near future and has envisioned a host of candidates from classical homogeneous and heterogeneous catalysts for which the presence of CO might actually be advantageous. (A final alternative to be discussed in detail at a later time is the use of a CO absorbing unit.) In the last quarter, Eastman initiated studies into the use of several homogeneous Ru- and Rh-based catalysts with little success to date.

Task 2.1 Direct Conversion of AcH and Ketene to VAM

a. Vapor Stripped (Small-Scale Reaction) Studies. Eastman examined the effect of furnace temperature on the VAM yield from ketene at otherwise fixed conditions (645 mmol acetic anhydride solvent, 30.6 mmol p-toluenesulfonic acid catalyst, 0.7 mmol ketene/min., 1.0 mmol acetaldehyde/min., 9.2 mmol N_2/min.). At 160°C, the VAM yields for consecutive days of operation were 45, 76, 82, 82, and 82% chronologically, and the heel contained 29 wt % EDA; at 150°C, corresponding VAM yields were 42, 75, 78 and 81 %, and the heel contained 29% EDA; at 140°C, corresponding VAM yields were 37, 75, 75, 75, and 80%, and the heel contained 39% EDA; and at 130°C, corresponding VAM yields were 37, 70 and 82%, and the heel contained 44 % EDA. The 130°C run was terminated prematurely due to equipment (refrigerated bath) failure. The data indicate that the effect of furnace temperature is small. The data also indicate that VAM yields from ketene using the straight acetic anhydride solvent are lower than those seen previously using the mixed acetic anhydride-acetic acid solvent system. However the yield does not drop off when the straight acetic anhydride system is used, whereas a yield drop-off is observed when the mixed acetic anhydride-acetic acid system is used.

b. Reactor Scaleup - Undiluted Feeds. Eastman constructed a unit for generating about 0.2-0.8 mol/h of ketene on a continuous basis. Over the last quarter, designs for separating ketene from by-product methane and CO were tested. (The ketene is currently being generated from acetone, accounting for the methane by-product.) The final separator consists of a condensing trap drained by a tube about 3 ft. long with a liquid trap (a U in the tube) to control addition. This separator is completely cooled with dry ice acetone. The reactor comprises a simple magnetically stirred cylindrical reactor with indentations to improve mixing. The ketene and acetaldehyde were bubbled into this reactor as a premixed gas (added via a mildly warmed line). The base of the reactor was filled with an EDA/acetic anhydride mixture containing p-toluene sulfonic acid as catalyst. The reactor was connected to a 15-plate Oldershaw Column. Product was removed via a splitter, and the operation was run using a 3/1 reflux ratio. The overall schematic appears below.

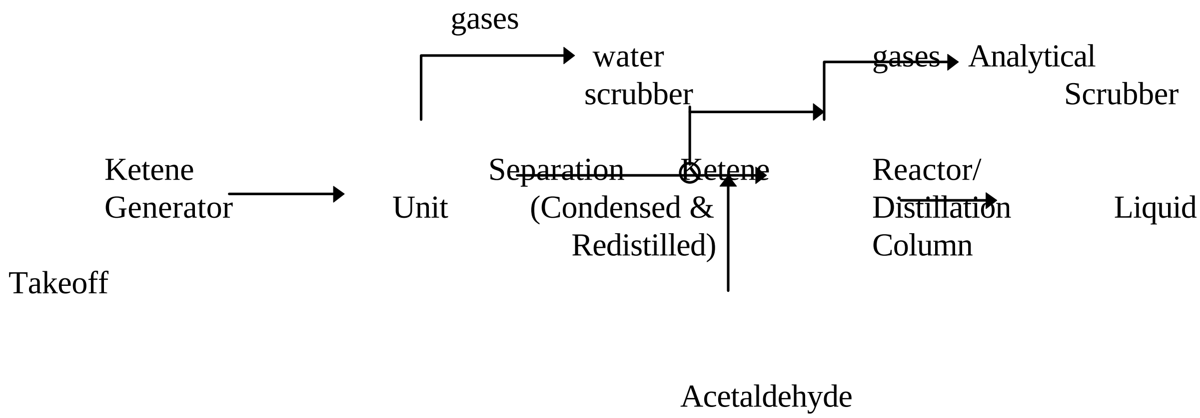

When initially calibrated using the methanol (analytical) scrubber, the separator delivered 0.413 mol/hr. However, when connected to the reactor, the separator efficiency was dramatically affected. Although Eastman completed a 3-day run, recalibrating by measuring the amount of ketene trapped as acetic anhydride in the column (using refluxing acetic acid at the same level at which the reactive distillation had been operated), the ketene introduction was reduced to 0.213 mol/h. Apparently, although the separator was built tall enough to compensate for pressure drops, the hydraulics of the reactor and distillation column still affected the separator's ability to deliver ketene.

Using the new calibration, Eastman was able to back out a material balance for the reaction which was surprisingly good given the large excess of acetaldehyde. The results of this run are provided in Table 3.2.10. Eastman will be pursuing this scaleup further, particularly with the generation and introduction of higher ketene levels with more closely matched acetaldehyde feeds.

Task 3.1.a. Assess Preliminary Economics for a Process Based on Ketene Hydrogenation. Eastman is continuing to assemble and adjust the models for each process needed to generate VAM from syngas. There is a great deal of interaction between the likely operating facilities, which continues to reduce the prospective cost. This work continues with several modules of the overall model well underway. Eastman's intent is to have a *preliminary* assessment available within the next quarter.

C. Summary of Plans for the Next Quarter

In the next quarter, Eastman plans to:

1. Continue its studies of the scaled-up version of the direct conversion of ketene and acetaldehyde to VAM.
2. Extend its examination of CO-tolerant catalysts (both homogeneous and heterogeneous) for the hydrogenation of ketene to acetaldehyde.
3. Initiate hydrocarbonylation studies for the direct conversion of methanol to acetaldehyde.
4. Continue to develop the economic models for the generation of VAM from syngas and a comparison with the conventional ethylene-based technology.
5. Complete the applicable patent portfolio covering this technology.

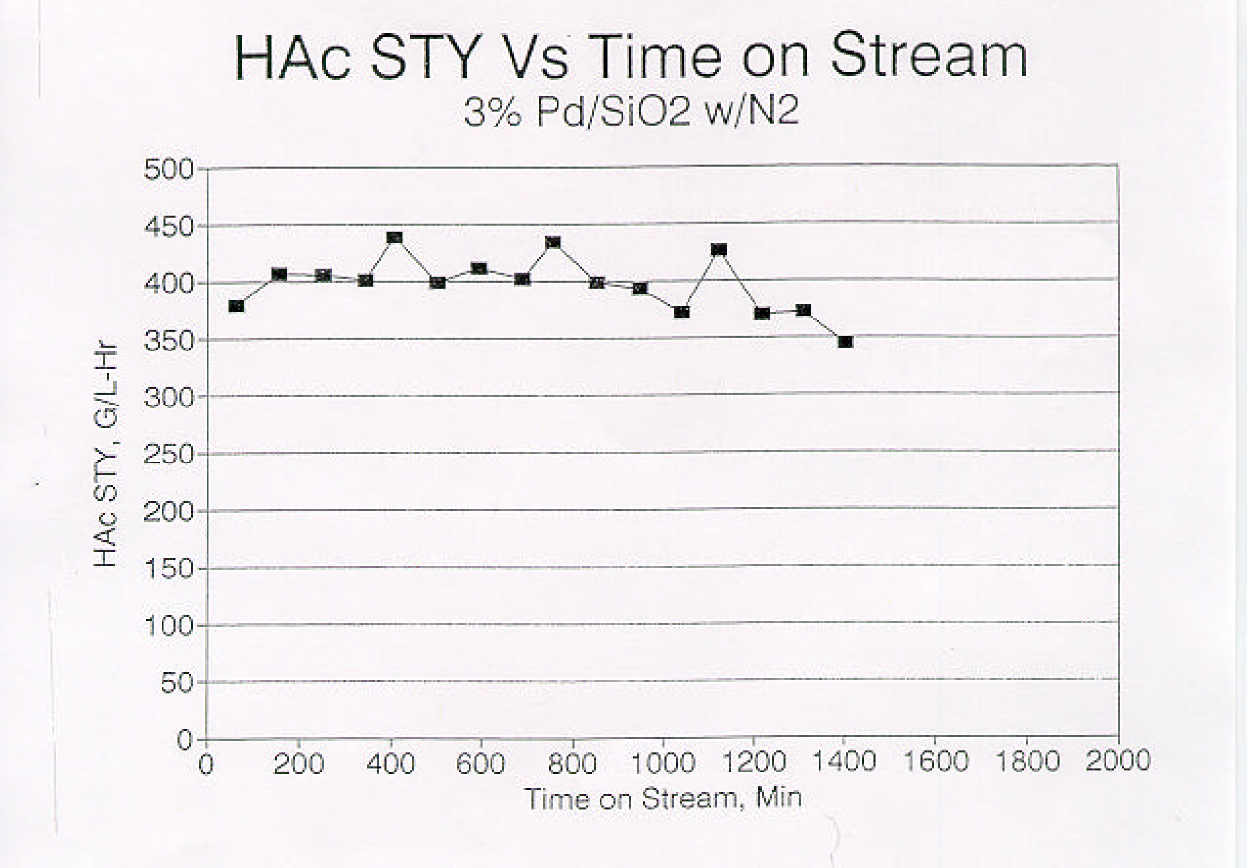
HAc STY Vs Time on Stream
3% Pd/SiO2 w/N2
HAc STY, G/L-Hr
500
450
400
350
300
250
200
150
100
50
0
0
200
400
600
800
1000
1200
1400
1600
1800
2000
Time on Stream, Min

Figure 3.2.1

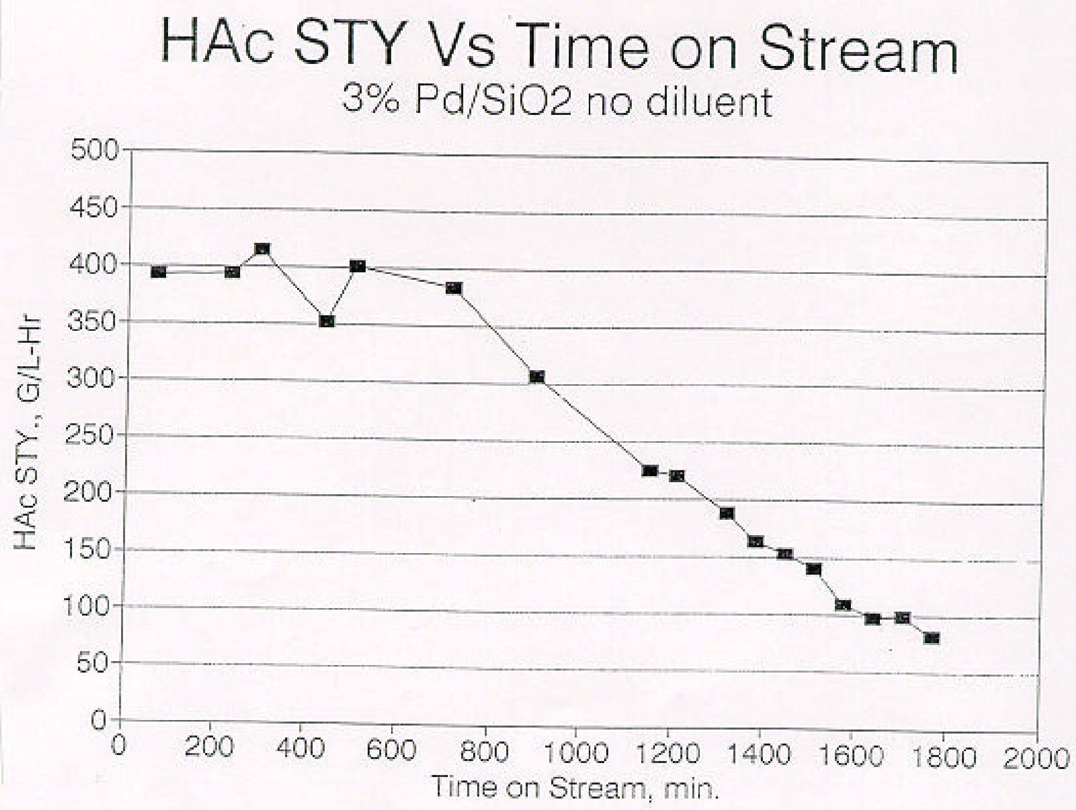
HAc STY Vs Time on Stream
3% Pd/SiO2 no diluent
HAc STY., G/L-Hr
500
450
400
350
300
250
200
150
100
50
0
0
200
400
600
800
1000
1200
1400
1600
1800
2000
Time on Stream, min.

Figure 3.2.2

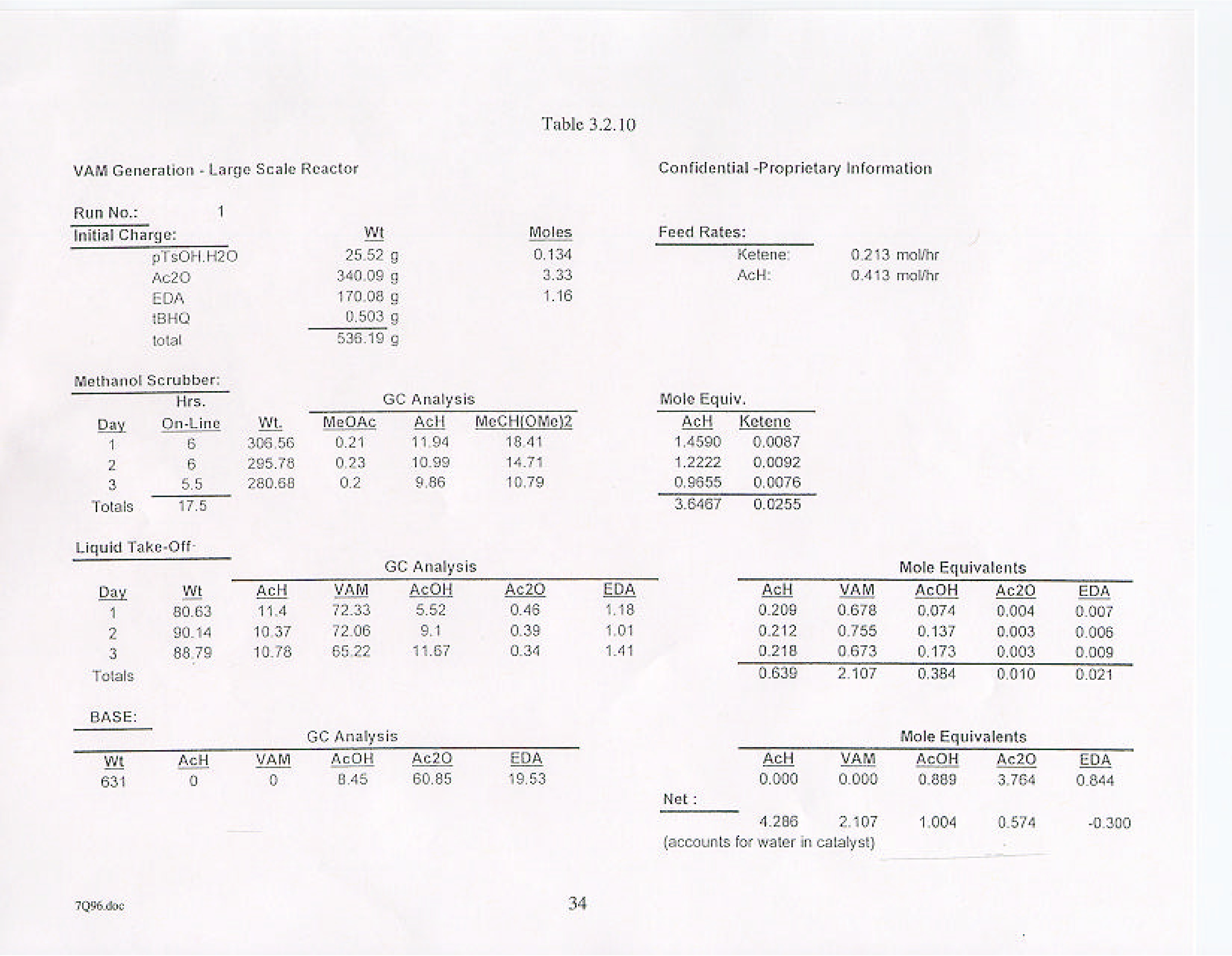

Table 3.2.10

VAM Generation - Large Scale Reactor

Confidential -Proprietary Information

Run No.: 1

Initial Charge:

	Wt	Moles
pTsOH.H2O	25.52 g	0.134
Ac2O	340.09 g	3.33
EDA	170.08 g	1.16
tBHQ	0.503 g	
total	536.19 g	

Feed Rates:

Ketene:	0.213 mol/hr
AcH:	0.413 mol/hr

Methanol Scrubber:

Day	Hrs. On-Line	Wt.	GC Analysis MeOAc	AcH	MeCH(OMe)2	Mole Equiv. AcH	Ketene
1	6	306.56	0.21	11.94	18.41	1.4590	0.0087
2	6	295.78	0.23	10.99	14.71	1.2222	0.0092
3	5.5	280.68	0.2	9.86	10.79	0.9655	0.0076
Totals	17.5					3.6467	0.0255

Liquid Take-Off-

Day	Wt	GC Analysis AcH	VAM	AcOH	Ac2O	EDA	Mole Equivalents AcH	VAM	AcOH	Ac2O	EDA
1	80.63	11.4	72.33	5.52	0.46	1.18	0.209	0.678	0.074	0.004	0.007
2	90.14	10.37	72.06	9.1	0.39	1.01	0.212	0.755	0.137	0.003	0.006
3	88.79	10.78	65.22	11.67	0.34	1.41	0.218	0.673	0.173	0.003	0.009
Totals							0.639	2.107	0.384	0.010	0.021

BASE:

Wt	GC Analysis AcH	VAM	AcOH	Ac2O	EDA	Mole Equivalents AcH	VAM	AcOH	Ac2O	EDA
631	0	0	8.45	60.85	19.53	0.000	0.000	0.889	3.764	0.844

Net :

	AcH	VAM	AcOH	Ac2O	EDA
	4.286	2.107	1.004	0.574	-0.300

(accounts for water in catalyst)

7Q96.doc

34

Task 3.3 New Processes for Alcohols and Oxygenated Fuel Additives

3.3.1 Isobutanol Synthesis in a Three Phase System

Slurry Reactor Design and Runs

Catalytic Runs

Based on two premises, the influence of the hydrodynamic residence time in the CSTR on the STY to isobutanol was investigated. The two premises are as follows:

- There are no mass transfer limitations under the conditions of isobutanol synthesis in a three-phase system.
- Yields of methanol and isobutanol are the same for a two- and a three-phase-system in the CSTR in terms of similarity in residence time and GHSV.

Experiments were made using the CSTR as a two-phase-system. The catalyst content was kept constant over all measurements while the mass flow of syngas was varied. The residence time was varied from 385 up to 1850 sec.

From experiments using the CSTR as a three-phase-system, it is known that an increase in catalyst loading causes a nearly linear increase in isobutanol at the reactor outlet (Figure 3.3.1).

Figure 3.3.1 Isobutanol in the Three Phase CSTR vs. Volume of Catalyst

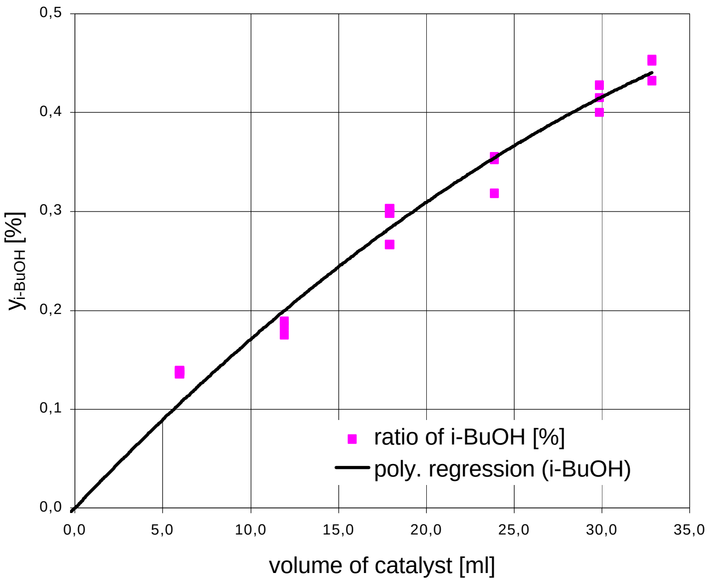

(p = 250 bar, ϑ = 400 °C, $\dot{V}_{\mathbf{Edukt}}$ = 115Nl/h, $ZnO/Cr_2O_3/K$-catalyst)

Increasing residence time causes a nearly linear increase in isobutanol (Figure 3.3.2). In both cases there is no influence of the partial pressure of isobutanol on the rate of reaction. Clearly, the isobutanol concentration is far from its equilibrium.

Figure 3.3.2 Isobutanol in the Two Phase CSTR vs. Residence Time

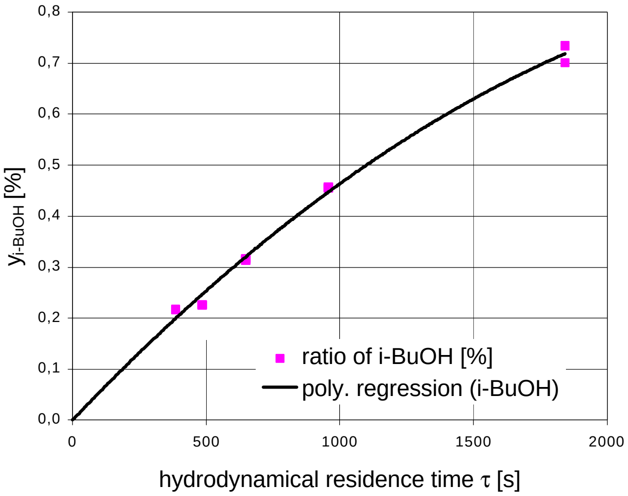

Time (p = 250 bar, ϑ = 400 °C, V_{kat} = 17,9 ml, ZnO/Cr_2O_3/K-catalyst)

Reactor Design Fluidized Bed

Heat transfer in a fluidized bed reactor from the fluid to the reactor walls and cooling coils was investigated further using a correlation of Martin[1]. Temperature and pressure were varied over a wide range (T = 400-700 K, p = 10-25 MPa), while the properties of the catalyst particles were kept constant (Table 3.3.1).

Table 3.3.1 Properties of the Catalyst Particles

diameter	d	[µm]	55
density	r_P	[kg/m³]	2027
heat capacity	c_p	[kJ/(kg·K)]	0.545

Significant changes in the properties of syngas by varying temperature and pressure occurred only in the case of density (Table 3.3.2). The thermal conductivity and the viscosity of syngas were nearly constant. Therefore, the density of the gas phase was the only free parameter and caused changes in the heat transfer coefficient "Fluid-Wall" h_{FW} (Figure 3.3.3). The heat transfer coefficient increased with decreasing density of syngas. Advantageous were high temperatures as well as low pressures.

---

[1] Martin, H., *VDI-Wärmeatlas*, Verein Deutscher Ingenieure (Editor), 7. Aufl., **1994**, Mf1-Mf8.

Table 3.3.2 Properties of Syngas (H_2/CO = 1) within the Temperature and Pressure Range (T = 400-700 K, p = 10-25 MPa)

density	r_g	$[10^{-3}$ kg/m³]	26 - 113
thermal conductivity	λ_g	[W/(m·K)]	0.149 - 0.156
viscosity	η_g	$[10^{-6}$ Ns/m²]	30.71 - 32.51
heat capacity	c_g	[kJ/(kg·K)]	1.981

Figure 3.3.3 Heat Transfer Coefficient h_{FW} vs. Temperature and Pressure

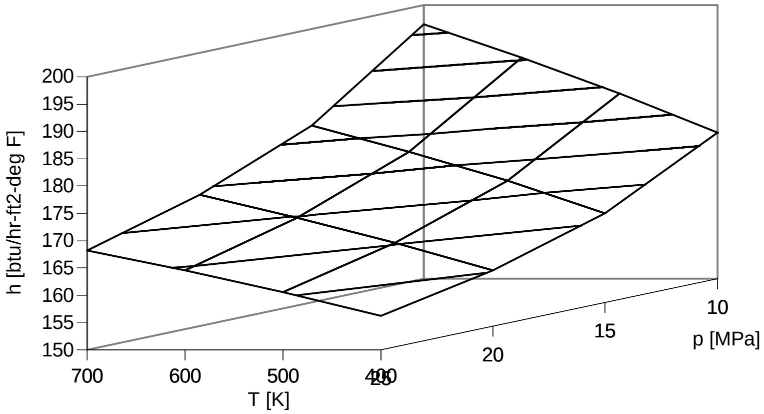

A better discussion on improving heat transfer in the fluidized bed reactor is possible by dividing heat transfer into three different mechanisms:

heat transfer coefficient:	**h =**	**h_p**	+	**h_g**	+	**h_r**
mechanism:		particle convection		gas convection		radiation

Heat transfer by radiation was low at the temperatures considered; for example, the heat transfer coefficient for a "black radiator" at a temperature T = 673 K is h_r = 12.2 Btu/hr-ft2-deg F. Therefore, the portion of heat transfer by radiation was ignored.

In the range of temperature and pressure mentioned above, the heat transfer by gas convection varied about 50%, while the heat transfer by particle convection was nearly constant (Table 3.3.3).

Figure 3.3.4 shows the influence of different synthesis methods on catalyst behavior. Three samples were tested with and without potassium promotion. Even in an unpromoted form, this system was a catalyst for isobutanol formation. Potassium promotion improved yields. However, the promoting effect was not similar for all three methods. Although total activities were essentially equal, clear differences in isobutanol yield were observed. The sol gel catalyst proved to be most active. Therefore this method was investigated in further detail.

Coprecipitation. As reported earlier (April-June 1994, January-March 1995), the initial goal of the work on coprecipitated Zr/Zn/Mn oxide catalysts aimed at optimizing the preparation parameters. In general the coprecipitated catalysts were prepared by precipitating the nitrate salts with potassium hydroxide at 80°C under constant pH conditions. The pH level during preparation mainly seemed to influence alkali content, leaving the composition unaffected. Thus, further investigation focused on examining the influence of the alkali metal. For this purpose, the following catalysts were compared:

Coprecipitated catalyst (Zr/Zn/Mn 1/1/1) with potassium hydroxide at pH 9:

- In its unpromoted state by removing potassium after precipitation through washing until no conductivity of the wash water was observed.
- After impregnating the aforementioned catalyst with 0.5 wt% potassium acetate (the optimum concentration; see quarterly report of January - March 1996).
- With alkali inclusion by incomplete washing after precipitation (see quarterly report of April - June 1994).

In addition, the last catalyst was impregnated with 0.25 wt% Pd (as described in the April - June 1994 quarterly report), which is known to enhance isobutanol activity.

The results are depicted in Figure 3.3.5. Catalysts were tested at 400, 425, and 450°C. All catalysts showed their optimum yield and selectivity for isobutanol at the highest temperature, the other major product being methanol.

Table 3.3.4 shows that the surface area varies greatly with a variation in catalyst composition. Generally the surface area seems to increase with increasing zirconia content. Pore size distribution shows a reciprocal behavior to surface area, that is, small pore sizes occur concomitantly with high surface area and vice versa.

Figure 3.3.6 Influence of Catalyst Composition on Isobutanol Activity and Selectivity

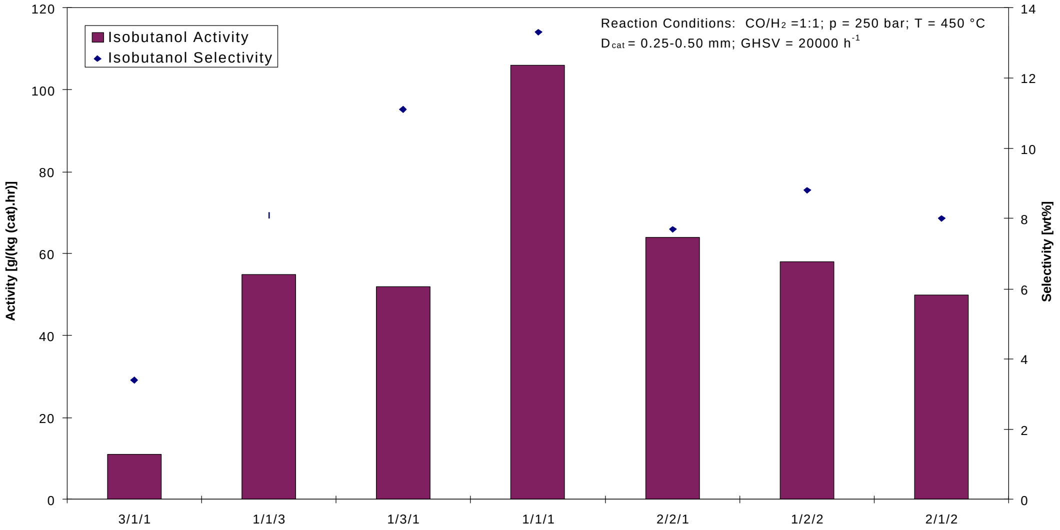

XRD plots indicate that no major crystalline phase is being formed during preparation or subsequent calcination. Only very ill-defined peaks belonging to zirconium oxide phases could be detected. Even calcination at 650°C did not change this behavior. The catalysis results are shown in Figure 3.3.6. For the unpromoted Zr/Zn/Mn oxide catalysts, an equimolar composition seems to be the best choice regarding activity as well as selectivity towards isobutanol.

However, a clear relationship between surface area or pore size distribution and isobutanol yield cannot be drawn from these data. Moreover, with an excess of zirconia (60%), it was observed that selectivity changes, and a major part of the product is shifted to dimethyl ether. This issue is being studied in more detail by changing surface concentrations of zinc and manganese oxide through impregnation on zirconia supports.

Sol Gel Methods. As described in earlier reports (January-March 1995, January-March 1996), the sol gel method offers a versatile route for the production of zirconium catalysts with new properties. This method allows the control of porosity and surface area by manipulation of the zirconium oxide network.

Tables 3.3.5 and 3.3.6 give an overview of the different types of catalysts with their surface characteristics.

Table 3.3.5 Synthesis Details for Different Sol Gel Catalysts

	Metal Salt	**Modifying Agent**	**Remarks**
NL72	nitrate	HOAc*[a]	no supercritical drying
NL73	nitrate	HOAc	
NL74	nitrate	HOAc	Zn/Mn salts added after gel formation
NL82	acetate	HOAc	
NL84	nitrate	HNO3[b]	acid catalyzed
NL90	nitrate	HNO3/acac[c]	acid catalyzed
NL102	nitrate	TMAH[d]	base catalyzed
NL99	nitrate	none	zirconium nitrate instead of alkoxide

[a] HOAc: acetic acid; [b]HNO3: nitric acid; [c]acac: acetylacetone; [d]TMAH: tetramethylammoniumhydroxide.

This synthesis method offers a way to change the porosity of a catalyst. The use of acetic acid as a modifying agent leads to the development of surface areas around 110 m^2/g, with pore sizes around 60 •, whereas the use of acetylacetone or base catalysis gives moderate surface areas with large pore sizes. Catalyst NL99 was made by just exposing a solution of the nitrates to a supercritical drying treatment. It can be seen that gel formation via the zirconium alkoxides seems to be important for the development of a large surface area.

Table 3.3.6 Surface Area and Pore Size Distribution of Different Sol Gel Catalysts

	Surface Area[a]	Max. Pore Size[b]
NL72	17	40
NL73	113	55
NL74	101	65
NL82	122	40
NL84	80	80
NL90	41	200
NL102	96	180
NL99	54	200

[a] in m^2/g (after calcination at 400 °C). [b] in •.

The catalysis results are depicted in Figure 3.3.7. The optimum for isobutanol production is found for catalysts with large surface areas and medium pore sizes. Interestingly, not only activity but also selectivity is enhanced for catalysts with this type of porosity. This behavior will be further investigated.

Figure 3.3.7 Isobutanol Activity and Selectivity for Different Sol Gel Catalysts

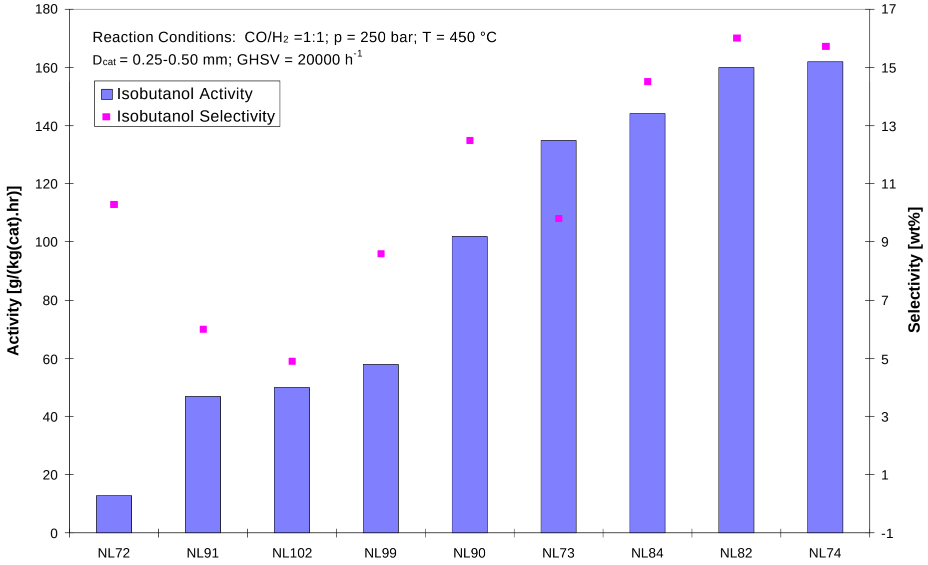

Future work will emphasize further optimization of the sol gel method, including post treatment, the influence of introducing alkali during gel formation and finally the addition of other elements such as rare earth metals as promoters.

Potassium-Promoted $ZrO_2/ZnO/Cu_2O$- Catalysts

The catalyst type presented in the last quarterly report was pointed out to be highly active at lower temperatures. Some test runs were performed in order to obtain detailed information about this catalyst.

Test Run 1

The catalyst was tested in the tubular reactor. It was calcined at 450°C (rate: 4°/min), keeping temperature constant for 3 hr. Catalyst reduction was done *in situ* with pure H_2 (30 bar) at 225°C (rate: 4°/min), keeping temperature constant for 2 hr.

The reaction was performed with syngas at 250 bar, increasing temperature from 340 to 430°C and then decreasing it to 340°C (Figures 3.3.8 and 3.3.9).

Figure 3.3.8 STY to Methanol and Temperature vs. Reaction Time in Test Run 1

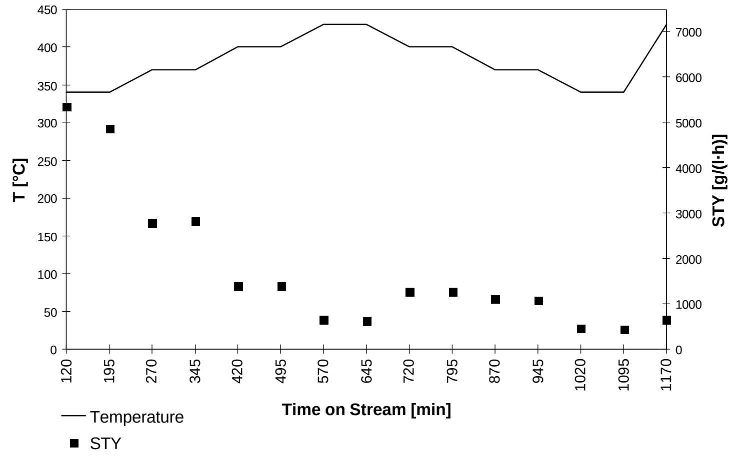

Figure 3.3.9 STY to Isobutanol and Temperature vs. Reaction Time in Test Run 1

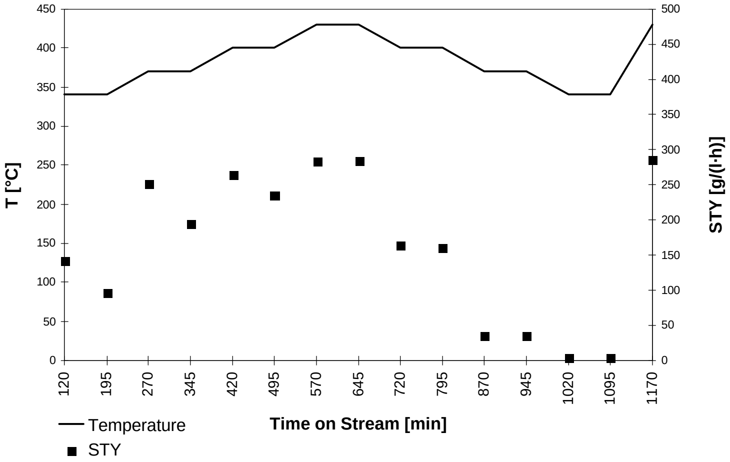

This test run showed that the catalyst was rapidly deactivating at low as well as at elevated temperatures.

Test Run 2

Because of this effect, a milder catalyst activation procedure was performed. This procedure involved overall heating rates of 1°/min. Reduction was carried out at 1 bar with a gas mixture of 30% H_2 and 70% N_2. A second test run in the tubular reactor was performed using this second catalyst. This catalyst deactivated too, but deactivation was less than for the first catalyst, especially when temperature was kept constant (Figures 3.3.10 and 3.3.11).

Figure 3.3.10 STY to Methanol and Temperature vs. Reaction Time in Test Run 2

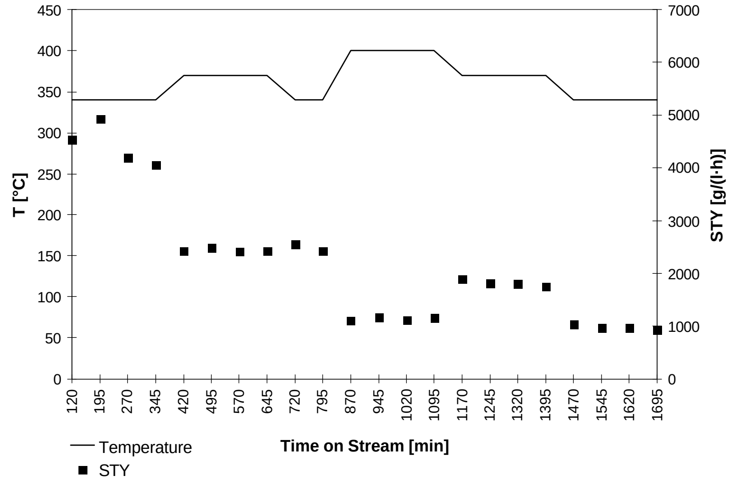

Figure 3.3.11 STY to Isobutanol and Temperature vs. Reaction Time in Test Run 2

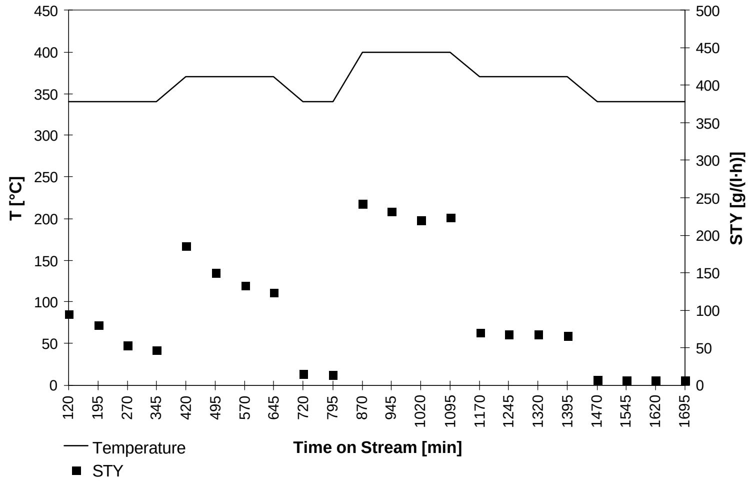

The catalyst used in test run 2 was analyzed by XRD, both after reduction and after reaction. In both cases, crystalline ZnO and copper could be identified. The only difference in XRD was in the lattice constant of copper. The lattice constant increased with the deactivated catalyst. This effect could be negated by further calcination and reduction (Figure 3.3.12), that is, the original lattice constant was obtained after a second calcination and reduction.

Figure 3.3.12 XRD Plot of the $ZrO_2/ZnO/Cu_2O$- Catalysts

a: copper after reaction
b: copper after reduction
c: ZnO in both cases

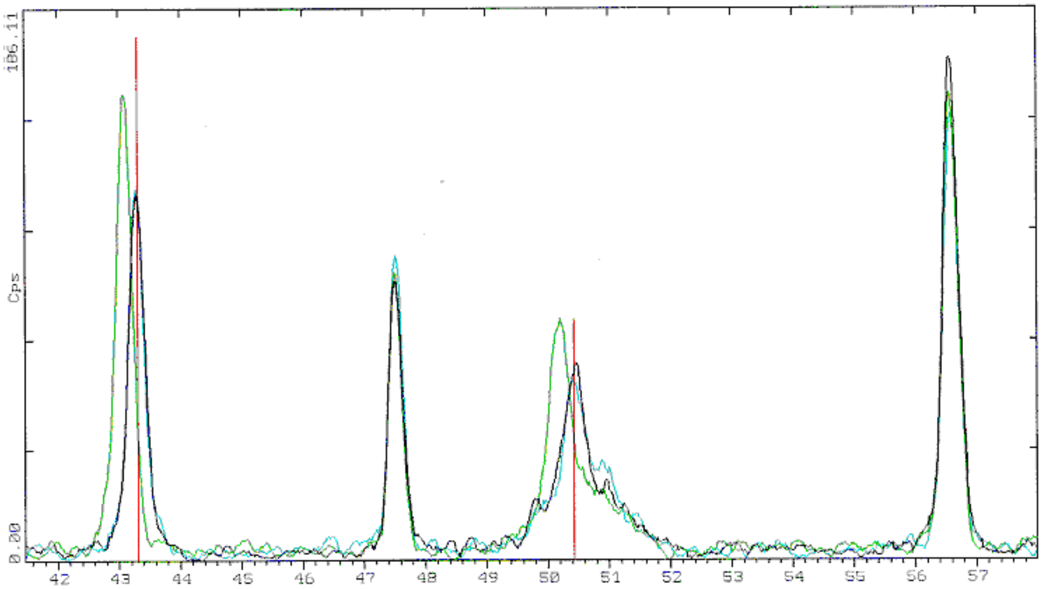

Further investigation is needed in order to determine if this is a thermal effect or an incorporation of hydrogen and, secondly, to clarify if this behavior is directly connected to the deactivation.

Test Run 3

The deactivation of the copper-containing catalyst underlined the importance of understanding and controlling temperature behavior in the catalyst bed. Therefore, a gradientless reactor for catalyst particles of different sizes was built.

This reactor, which is a kind of spinning basket reactor, consists of a small basket that is placed in the CSTR and is connected with the stirrer shaft. This allows the measurement of reaction parameters without gradients in temperature and gas composition over the catalyst bed.

In order to compare catalyst behavior, a first run was performed with the catalyst used in the tubular reactor in test run 2 (Figures 3.3.13 and 3.3.14).

Figure 3.3.13 STY to Methanol and Temperature vs. Reaction Time in Test Run 3 (Gradientless)

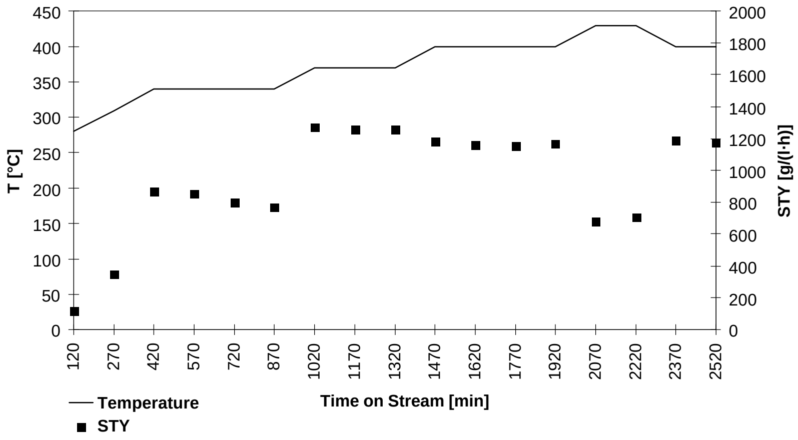

Figure 3.3.14 STY to Isobutanol and Temperature vs. Reaction Time in Test Run 3 (Gradientless)

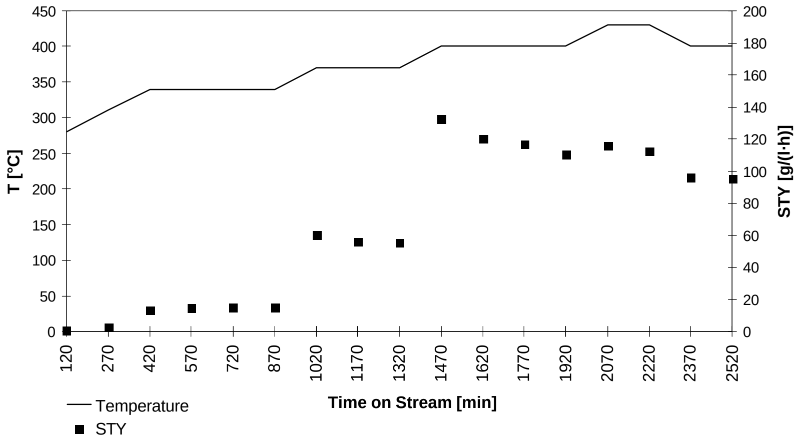

The deactivation decreased with the gradientless reactor. An explanation might be that deactivation takes place during temperature overshots in the catalyst bed, which are common in fixed bed reactors, but do not occur to this extent in gradientless reactors.

3.4 Chemicals from Synthesis Gas - No progress to report this quarter.

3.5 Poison Resistant Catalyst Development and Testing

3.5.1 Alternate Fuels Field Test Unit (AFFTU)

The AFFTU was first used for feedstock testing for the LPMEOH™ Demonstration Facility under construction at Eastman Chemical’s Kingsport, Tennessee plant. The AFFTU was partially disassembled at the Air Products lab site, transported to Kingsport, and reassembled. The unit arrived in very good condition and was fully operational as scheduled, after three days of setup and checkout. An Operational Readiness Inspection of the AFFTU and the associated tie-ins to Eastman's process equipment was performed.

Two simultaneous tests lasting four weeks were conducted at Eastman: [1] a life-test of the LPMEOH™ reaction using Eastman's syngas and the AFFTU's 300-mL reactor and [2] continual monitoring of the feed composition. The objective of this part of the study was to both identify concentrations of poisons in the feed and to test their removal by various combinations of four guard beds (also located in the AFFTU).

Methanol productivity over the course of the testing is shown in Figure 3.5.1. The two primary feeds to the LPMEOH™ Demonstration Facility were used as feed to the AFFTU. A blend of 75% balanced syngas and 25% makeup CO was chosen to allow the maximum sensitivity to possible contaminants in either feed while remaining within the envelope of feed mixtures to be used for the actual plant.

The results of poisons monitoring in the fresh syngas feed (upstream of the guard beds) are shown in Figure 3.5.2. The four guard beds tested contained methanol synthesis catalyst, Y Zeolite, activated carbon and a commercial arsine adsorbent, respectively. For the first 4½ days of operation, all four beds were used in series. The beds were removed from the feed stream in the following sequence: arsine adsorbent, Y Zeolite, methanol synthesis catalyst and activated carbon. The system was run with the activated carbon bed alone for four days to evaluate the impact of carbonyl sulfide (which passed through the carbon bed) on the catalyst while iron and nickel carbonyl were removed. The carbon bed was then removed, inaugurating a period of 18 days of actual onstream operation without any guard beds.

Significant events during the run are listed in Table 3.5.1. Note that on two occasions, Eastman's syngas supply was interrupted. The first outage lasted 18 hours; the second lasted over 4 days.

The most significant findings of this work were that:

1. No poisons were present in Eastman's "balanced syngas" or "makeup CO" streams in sufficient quantities to cause deactivation of the catalyst at a rate distinguishably faster than normally observed in the laboratory using "clean" feed. Figures 3.5.3 and 3.5.4 show the results of linear regression of various portions of the methanol productivity history. The slopes calculated for these lines compare favorably with those previously measured in 300-mL laboratory autoclaves using "Kingsport Gas." Those runs typically showed 0.020 - 0.025 %/hr productivity loss. Although in Figure 3.5.4 the rate of productivity loss after removal of the adsorbent beds *appears* somewhat faster than that observed before the removal of the carbon bed (0.017%/hr versus 0.007%/hr), all of this activity loss occurred in a single step change at 390 hours. The cause of this step change is not known. Otherwise there appears to be no evidence of an increased rate of activity loss in the absence of feed pretreatment.

   The apparent decrease in methanol synthesis activity over the first 50 hours of the experiment was most likely due to: (1) GC calibration drift (note the recalibrated data after 160 hours on stream) and/or (2) an initial period of hyperactivity that we have occasionally observed in previous laboratory experience. In either case, the cause is not related to the presence of poisons in the reactor feed.

2. Carbonyl sulfide (<25 ppb) and hydrogen sulfide (<10 ppb) were observed during normal syngas generation. This level of sulfur falls comfortably within the specification provided by Air Products Process Engineering (60 ppb total sulfur). Higher levels (up to 190 ppb) were seen briefly after the second re-start of Eastman's gasifiers (Figure 3.5.2); total sulfur was back within specification after 2½ hours, and COS was below 30 ppb after 10 hours. This indicates that under typical operating conditions, sulfide is not a problem, but that there would be value in monitoring the sulfide content of the feed gas on restart of the gasifiers before the LPMEOH™ plant is put back on line to avoid unnecessary exposure of the catalyst to sulfide.

3. The presence of nickel carbonyl in the feed gas mix (Figure 3.5.2) was demonstrated to be an artifact of the tie-in between Eastman's piping and the AFFTU. This conclusion is based on two observations. First, the concentration of nickel carbonyl gradually decreased from initial levels of 100-300 ppb, and eventually nickel carbonyl was not observed at all. Second, when the flow rate through the tie-in tubing was tripled, a step change decrease in the nickel carbonyl concentration was seen. Iron carbonyl was shown to be mostly, if not completely, an artifact. The possibility that some iron carbonyl is actually present in Eastman's gas cannot be ruled out because (1) unlike nickel, the iron was not eventually depleted and (2) tripling the flow rate through the tie-in resulted in only a 35% decrease in the iron carbonyl concentration (from 5.1 to 3.3 ppb -- see Figure 3.5.2, 10.6 days). Although these observations can certainly be consistent with *all* of the iron coming from the tie-in, they could also be explained by the presence of up to roughly 2.5 ppb iron carbonyl in Eastman's gas.

4. A 12% loss in productivity was observed over the course of the second gasifier outage. It is most likely that the idle period itself, and not poisons in the feed stream, was the cause of the activity loss. This conclusion stems from two points. First, during the initial 12 hours of the idle period, the reactor was accidently left at 250°C; only after that time was the reactor cooled to 200°C. It has been shown that idling the catalyst under syngas at 250°C does lead to deactivation. Second, although there was a COS excursion on re-start, the cumulative exposure to sulfide between the outage and the first activity test that followed (even accounting for the idled time) was only about 35% of the cumulative exposure during the previous 14 days, during which only 4% deactivation was observed. Therefore it is very unlikely that the 12% productivity loss during the outage was due to COS poisoning. We are awaiting the results of elemental analysis on the spent catalyst to determine whether any other compounds may have accumulated on it.

5. The life test began with four guard beds in place: (1) crushed pellets of S3-86, (2) UOP LZY-72, (3) BPL carbon and (4) UCI G-132D arsine adsorbent. Initially, all of the poisons were removed by Bed #1. After a few days, nickel carbonyl broke through Bed #1 and, subsequently, Bed #2; however, Bed #3 (BPL carbon) provided complete nickel

carbonyl removal until it was removed on day 10. Samples drawn 3 in. from the feed end of this bed did not reveal the presence of any nickel carbonyl, showing the effectiveness of the carbon in nickel carbonyl removal. A small amount of carbonyl sulfide also passed through Bed #1, but only to a level of 0.5 ppb; most of the COS was still removed by Bed #1. This 0.5 ppb passed untouched through to the autoclave. Bed #4 was dropped on Day 4 and Bed #2 was dropped on Day 5. No significant changes in methanol synthesis activity or poisons concentrations were observed. Bed #1 was dropped on Day 6; this allowed the full trailer feed concentration of COS (7-16 ppb) to reach the autoclave. Since this poison is actually present in Eastman's gas (not an artifact of the tie-in procedure), we extended this phase of the experimental program to four days to assess the impact of this level of COS on catalyst stability (iron and nickel carbonyl and hydrogen sulfide were still removed by Bed #3). No discernible change in methanol synthesis activity was observed.

Table 3.5.1 Run Event History

Event	Date & Time	Time Onstream[1]	Days of Operation[2]
Beginning of Run	5/15 1440	0	-0.35[3]
Bed #4 Dropped	5/20 830	114	4.40
Bed #2 Dropped	5/21 930	139	5.44
Bed #1 Dropped	5/22 1000	163	6.56
Bed #3 Dropped	5/26 1500	264	10.67
First Gasifier Outage	5/30 1430	360	14.65
Restored	5/31 400	360	15.21
Second Gasifier Outage	6/6 730	503	21.36
Restored	6/10 1000	503	25.47
Run Terminated	6/17 1700	678	32.68

---

[1] Stability Data – time in hours on stream. Periods where the reactor is not receiving syngas feed and at temperature are considered downtime and "hours on stream" are not accrued during this time (note the two gasifier outages).

[2] Poisons Data and Graphs -- time in Days, reactor downtime included.

[3] This negative value results from having accidentally chosen slightly different times as the starting point for the stability and poisons spreadsheets. Since these two spreadsheets count downtime differently and therefore cannot be compared side by side, I have not chosen to reconcile their start times.

Figure 3.5.1 Methanol Productivity during Testing

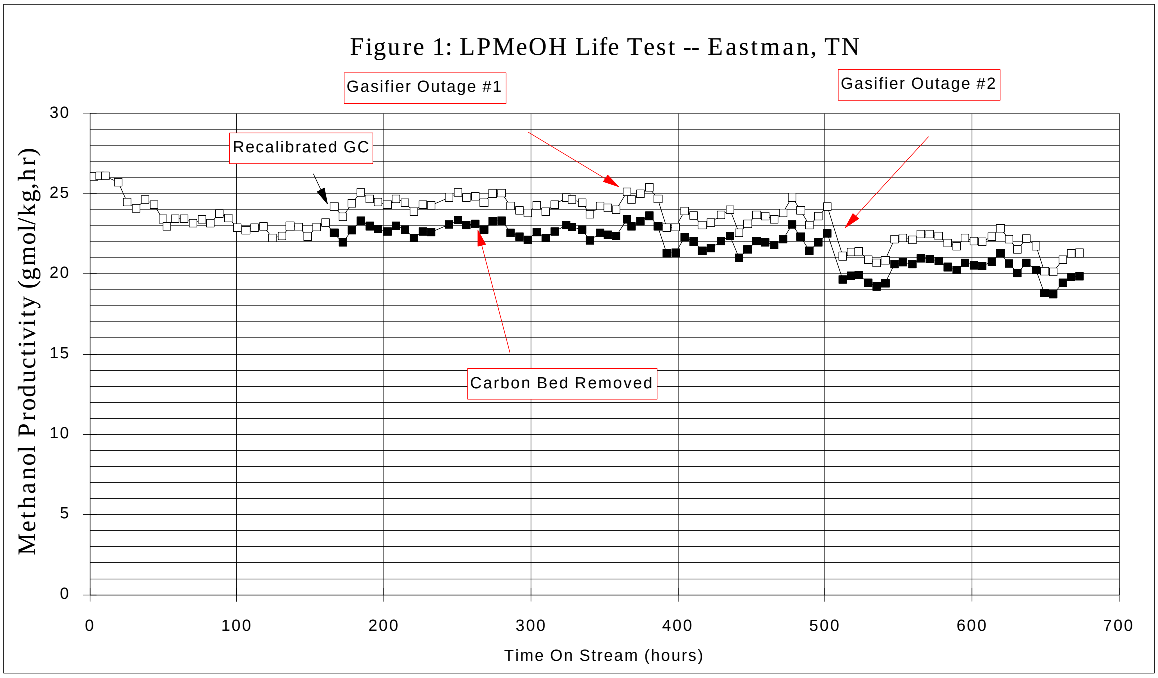

Figure 3.5.2 Poisons Monitoring

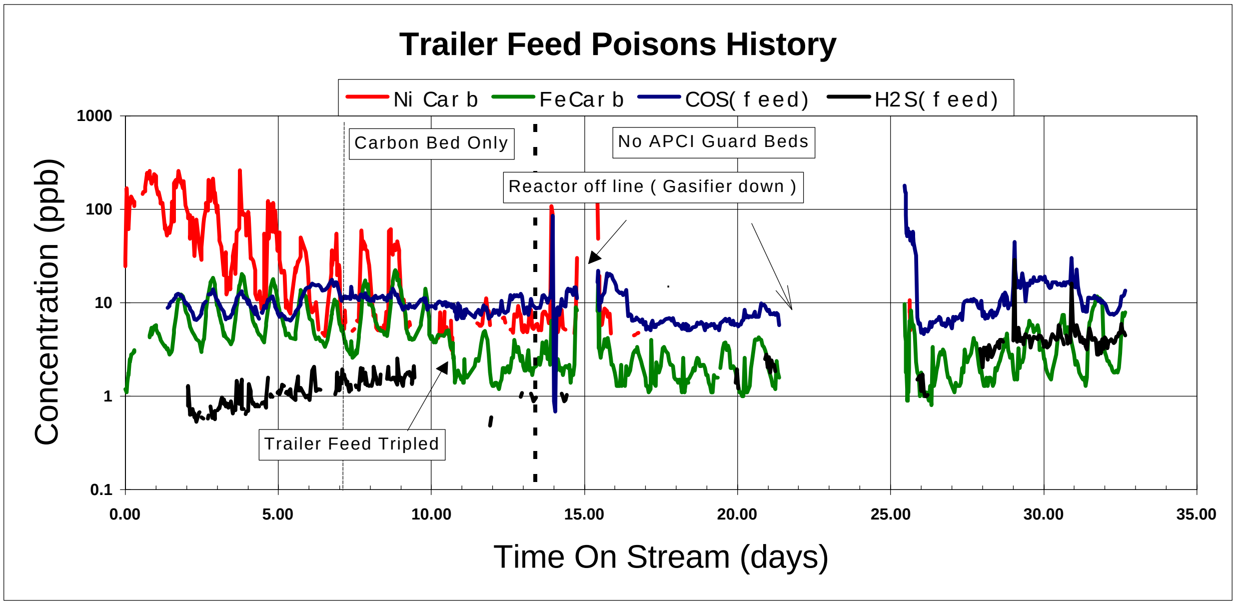

Figure 3.5.3

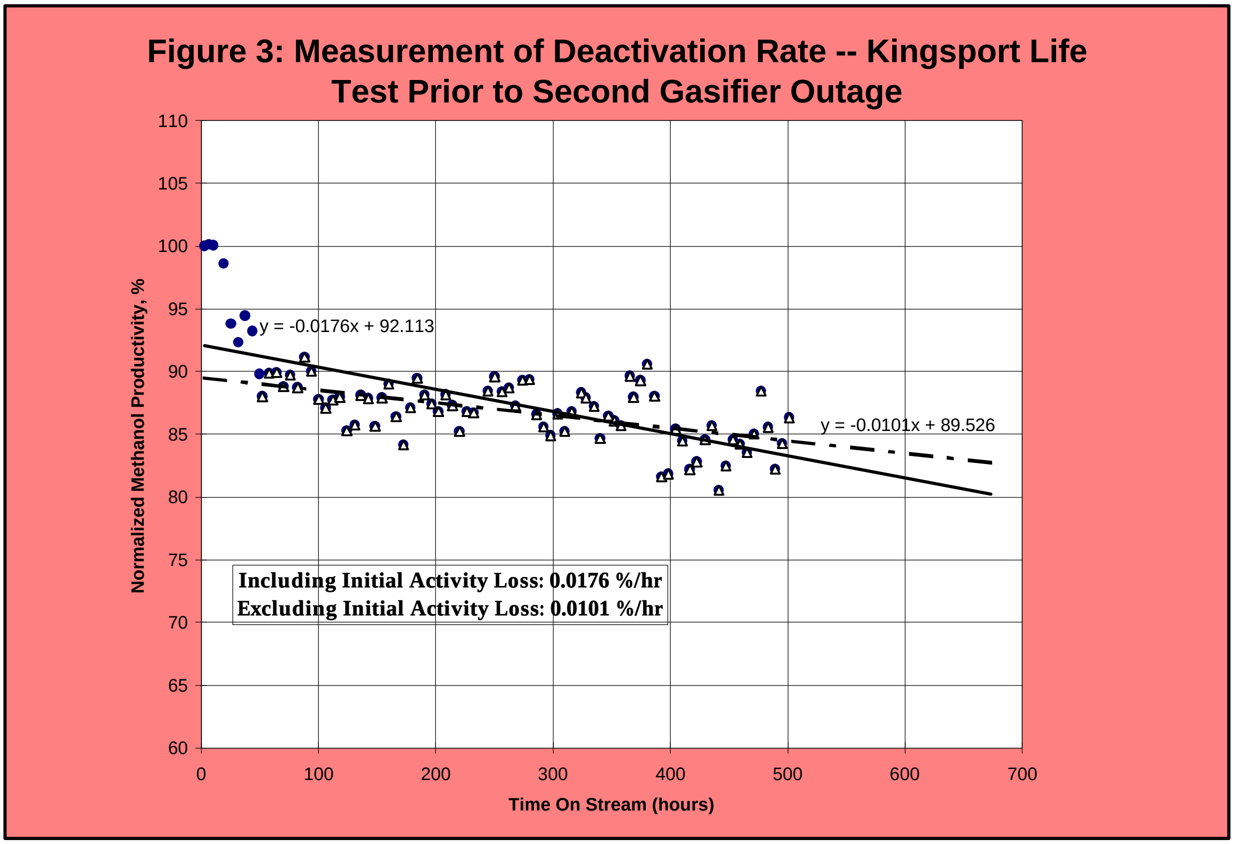

● - all data
Δ - data after initial period of rapid activity loss
(these two data sets yield the average activity loss rates shown in the figure)

Figure 3.5.4

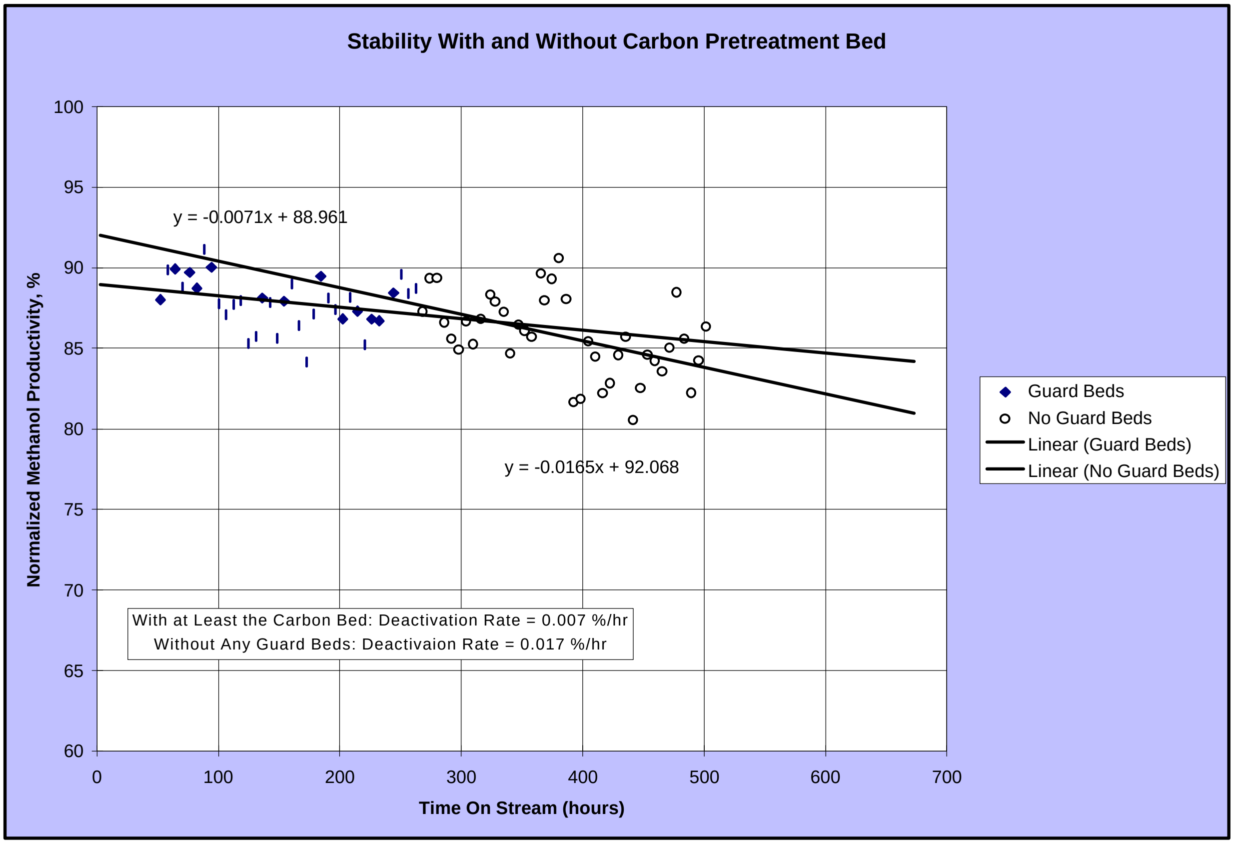
Stability With and Without Carbon Pretreatment Bed
y = -0.0071x + 88.961
y = -0.0165x + 92.068
With at Least the Carbon Bed: Deactivation Rate = 0.007 %/hr
Without Any Guard Beds: Deactivaion Rate = 0.017 %/hr
Normalized Methanol Productivity, %
100
95
90
85
80
75
70
65
60
0
100
200
300
400
500
600
700
Time On Stream (hours)
Guard Beds
No Guard Beds
Linear (Guard Beds)
Linear (No Guard Beds)

TASK 4: PROGRAM SUPPORT

In April, Bechtel made presentations on mixed alcohol synthesis (Task 4.2) and on the economic incentive for sulfur removal (Task 4.5) at a DOE project review meeting at Air Products' Allentown offices. Under Task 4.2, for all three scenarios for the production of gasoline blendstock ethers via liquid phase mixed alcohol synthesis (LPMAS), economical LPMAS plants are possible, even at current (low) ether market prices. However, large improvements in catalyst productivity and alcohol selectivity must be achieved before commericalization of this process. Furthermore, if inexpensive natural gas feedstock is available, coproduction of methanol and ethers appears attractive because of less demanding catalyst productivity and selectivity requirements. Under Task 4.5, Bechtel presented the results of the preliminary study examining the cost savings realized by relaxing the sulfur removal specification from <0.1 ppmv total sulfur in the treated syngas to 20 ppmv total sulfur for four different syngases, each using a different sulfur removal technology. The primary basis for this study is a coal-based production facility rated at 1660 stpd of methanol. The cost saving, which is realized through design differences in the sulfur removal plant, is the metric by which catalyst developers/manufacturers can determine if there is sufficient incentive to develop sulfur-tolerant catalyst. This cost savings was evaluated at between $3 and $5 million a year for the different cases, indicating that an economic incentive to develop a sulfur-tolerant catalyst may exist.

During May, work consisted mainly of report and paper preparation to document technical and economic results:

- Under Task 1.3, Fischer-Tropsch Support, the final version of the topical report entitled "Fischer-Tropsch Wax/Catalyst Separation Study" was issued. This report describes the catalyst separation technique study conducted by Bechtel.
- Under Task 4.2, a draft topical report on the results of the study of three scenarios for the production of gasoline blendstock ethers via LPMAS was issued. A summary of the study entitled "Economics of MTBE Production from Synthesis Gas" was submitted to DOE as a paper to be presented at the July 1996 First Joint Power and Fuel Systems Contractors Conference.
- Under Task 4.5, information on the study to evaluate the economic incentive to develop a sulfur-tolerant methanol synthesis was provided for the first quarter 1996 report to DOE. Work on preparation of a draft report on this study and on the report on the identication of trace contaminants in syngas and the systems to remove them was delayed due to budget constraints and emphasis on other work.

In June, work was initiated on a study under Task 4.2 to develop the cost of production of dimethyl ether (DME) from synthesis gas using Air Products' slurry phase process. A preliminary design basis and work scope were prepared for several different utilization schemes. Preliminary DME/methanol equilibrium calculations for some nominal syngas compositions were performed to develop insight into the process requirements. In addition, materials were prepared for the presentation of results of the study entitled "Economics of MTBE Production from Synthesis Gas" at the July 1996 PETC Contractors Conference. Under Task 4.5, work on preparation of draft reports on 1) the study to evaluate the economic incentive to develop a sulfur-tolerant catalyst, and 2) identification of trace contaminants in syngas and systems to remove them was continued at a reduced level due to budget constraints.

TASK 5: PROJECT MANAGEMENT

5.1 Reports and Presentations

Monthlies for April, May and June were issued, and a draft quarterly for April through June 1996 was in preparation.

Liquid Phase Hydrodynamic Run

A meeting was held with Sandia personnel to discuss results of the hydrodynamic run and to plan sparger studies at Sandia. Efforts continue toward writing joint papers from this work. Further analysis of the run was presented at a DOE review meeting in Allentown by Air Products, Sandia, and Washington University personnel. The presentations generated keen interest in continuing the fluid dynamics work. Differential pressure measurements are already planned for the F-T III run, while tracer studies are now being reconsidered for inclusion in the scope.

A paper entitled "Recent Results from LaPorte Alternative Fuels Development Unit" was completed. The paper, co-authored by Air Products and Sandia personnel, discusses results from the 1995 Hydrodynamic/LPMEOH™ run. It will be presented at the First Joint Power and Fuel Systems Contractors Conference in Pittsburgh (July 9-11,1996).

5.2 Management Activities

In the work on acetyls at Air Products, three U.S. patents were filed on 21 May 1996, and the titles are provided below:

1) Heterogeneous Catalyst for the Production of Ethylidene Diacetate from Dimethy Ether.
2) Heterogeneous Catalyst for the Production of Ethylidene Diacetate from Acetic Anhydride.
3) Heterogeneous Catalyst for the Production of Acetic Anhydride from Methyl Acetate.